

Chapter 6

Auger Electron Spectroscopy

When a vacancy is formed in one of the inner shells of an atom, it may be filled by either a radiative (x ray) or nonradiative (Auger) process. In most instances nature chooses the Auger process. Only when the transition energy exceeds roughly 10 keV is x-ray emission predominant. Thus, the fluorescence yield is greater than 0.5 only for vacancies in the K shells of atoms whose $Z > 30$, and in a few cases in the L shell for very heavy elements. (The fluorescence yield ω is defined as equal to the number of times a vacancy in a given shell is filled by a radiative process divided by the total number of times that hole is filled.) Why, then, are x rays well known even to the man in the street, while the understanding of the Auger processes has been until recently restricted to the specialist? The answer lies simply in the ease of measurement. X rays are a highly penetrating radiation, while Auger electrons have only a small mean free path in solids.

The Auger process was discovered by Pierre Auger⁽¹⁾ (pronounced *oh jay'*) using a Wilson cloud chamber. Tracks corresponding to ejected electrons could be seen along a beam of x rays. An Auger event could be detected by the presence of a double track emanating from a single source. One track was due to photoelectron ejection, while the second was due to the ejected Auger electron. The Auger effect has been of interest to the x-ray spectroscopist because of its profound influence in altering the fluorescence yield, or in broadening the natural width of the x-ray lines by shortening the lifetime of the vacancy state. For a review of x-ray fluorescence yields, together with Auger and Coster-Kronig transition probabilities, see Bambynek *et al.*⁽²⁾ Nuclear spectroscopists have also needed to study the Auger process in order to better account for their data on electron capture and internal conversion in which inner shell vacancies are being promoted. If, for example, the probability for K capture for a given element is being monitored by the number of x rays observed, then the fluorescence yield needs to be known. In the study of

internally converted electrons, beta spectroscopists also measure the discrete-energy Auger electrons.

For the most part, the early studies of the Auger process were studies of a nuisance effect. One needed to know about it in order to correct one's data, but the effect was not of too much intrinsic value. The Auger effect did shed light on atomic processes, such as the type of coupling ($LS, j-j$, or intermediate) throughout the periodic table; but, in general, relatively little constructive use was made of the phenomenon. In the last few years this situation has changed drastically. Two media in which the collision cross section does not prevent the detection of even low-energy Auger electrons are gases and surfaces. The study of Auger electrons under these conditions has proven to be most profitable.

Studies of Auger electrons in gases have been useful in learning about the basic phenomenon of ionization and about the nature of molecular ions, while in the study of surfaces, Auger spectroscopy has been invaluable as an analytical tool. In this chapter we shall discuss in detail some of the more recent applications of Auger spectroscopy in both gases and solids. But before doing so, we must pass on to a more thorough discussion of the phenomenon itself.

1. THEORY OF THE AUGER PROCESS

The first book to discuss the basic phenomenon of the Auger effect was by Burhop.⁽³⁾ Other excellent reviews are by Mehlhorn,⁽⁴⁾ Sevier,⁽⁵⁾ Parilis,⁽⁶⁾ and Burhop and Asaad.⁽⁷⁾

A nonradiative readjustment to an inner shell may take place by having one electron from a less tightly bound orbital fill the hole, while a second electron is ejected into the continuum with an energy equal to the difference in total energies of the initial and final states. For example, take the $K-L_1L_{II}$ Auger transition. The initial state has a hole in the K shell, and the final state has two vacancies in the L shell. Symbolically, we represent the Auger process by the naming of the orbitals or shells in which vacancies occur, both in the initial state (in our example, the K shell) and the final state (the L_1 and L_{II} subshells). Energetically, this is equivalent to producing a virtual $K-L_{II}$ x ray that photoejects an electron from the L_1 shell. However, this is not the way an Auger process occurs. It is rather a two-electron Coulombic readjustment to the initial hole. This is shown by the presence of the $1s-2s2s$ Auger process. A $1s-2s$ radiation process is not allowed in the dipole approximation.

The energy of an Auger electron E_A can be estimated from the binding energies, e.g., for a $K-L_1L_{II}$ Auger process

$$E_A = E_K - (E_{L_1} + E'_{L_{II}}) \quad (6.1)$$

where E_K and E_{L_1} are the binding energies of the K and L_1 shells of a neutral atom and $E_{L_{II}}'$ is the binding energy of an electron in the L_{II} shell of an ion having a single vacancy in the L shell. The binding energy for a given shell in an ion having a single-hole configuration is slightly larger than that for its atomic counterpart. Bergström and Hill⁽⁸⁾ suggested $E_L' = E_L(Z + \Delta Z)$, where $E_L(Z + \Delta Z)$ is the binding energy of an electron in shell L lying between those for atoms with atomic numbers Z and $Z + 1$, where $0 < \Delta Z < 1$. For example, E_L' for Z around 80 has $\Delta Z = 0.55$. Atomic binding energies are available both experimentally and theoretically, so that equation (6.1) may be used to obtain an estimate of the Auger transition energy. Coghlan and Clausing⁽⁹⁾ have published a complete listing of Auger energies for elements up to $Z = 92$, using the approximation

$$E_A = E_X - \left\{ \frac{1}{2}[E_X(Z) + E_X(Z + 1)] + \frac{1}{2}[E_Y(Z) + E_Y(Z + 1)] \right\} \quad (6.2)$$

Packer and Wilson⁽¹⁰⁾ also have a comprehensive listing, but based on a less reliable approximation. Shirley⁽¹¹⁾ has considerably improved the estimates of Auger energies by consideration of relaxation effects, and Nicolaides and Beck⁽¹²⁾ have examined the requirements for an "exact" calculation of KLL Auger energies. Comprehensive listings of experimental Auger energies are given by Siegbahn *et al.*,⁽¹³⁾ in a chart put out by Varian,⁽¹⁴⁾ and in a collection of spectra measured by Palmberg *et al.*⁽¹⁵⁾

A more detailed treatment of the Auger energies requires knowledge of a coupling in the final state which occurs between the two unfilled shells. For light elements the coupling scheme is pure $L-S$, for heavy atoms $j-j$, and for elements in the middle of the periodic table intermediate coupling needs to be invoked. Figure 6.1 shows the Auger lines that can arise from $K-LL$ Auger transitions. For the light elements there are five lines (the $1s-1s2p\ ^3P$ transition is forbidden according to the $L-S$ coupling scheme). Pure $j-j$ coupling yields six lines, while in the intermediate region as many as nine lines are allowed and can be discerned.

Let us next turn our attention to the calculations of the Auger transition probability, which is given as

$$P_{i \rightarrow f} = \frac{2\pi}{\hbar} \left| \int \int \chi_f^*(\mathbf{r}_1) \psi_f^*(\mathbf{r}_2) \frac{e^2}{|\mathbf{r}_1 - \mathbf{r}_2|} \chi_i(\mathbf{r}_1) \psi_i(\mathbf{r}_2) d\mathbf{r}_1 d\mathbf{r}_2 \right|^2 \quad (6.3)$$

The two electrons involved are initially in bound orbitals represented by χ_i and ψ_i . Following the nonradiative Coulombic readjustment, the final states of the electron are represented by a bound orbital χ_f^* (the filled vacancy) and the continuum wave function ψ_f^* , which is normalized to represent one ejected electron per unit time per unit energy range. When account is taken of the fact that the initial and final wave functions must be antisymmetric in their coordinates, one has expressions due to direct ($\chi_i \rightarrow \chi_f$; $\psi_i \rightarrow \psi_f$) and exchange

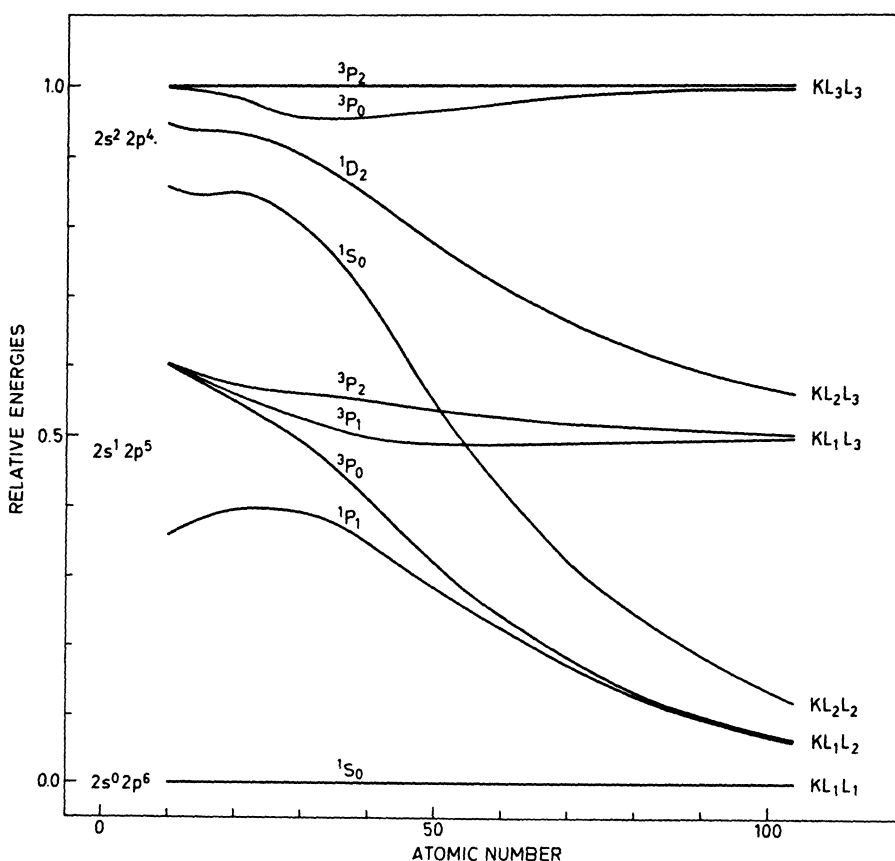


FIGURE 6.1. Relative line positions in $K-LL$ Auger transitions as a function of Z . At low Z one has nearly pure $L-S$ coupling and six lines. However, the $2s^2 2p^4 \ ^3P$ is strongly forbidden in the nonrelativistic region. At high Z one has nearly pure jj coupling and six lines; nine lines are possible in the intermediate coupling region. [Reproduced from Siegbahn *et al.*,⁽¹³⁾ Figure 4.1.]

$(\chi_i \rightarrow \psi_f; \psi_i \rightarrow \chi_f)$ transitions. Another theoretical approach to Auger transition has been given by Haymann,⁽¹⁶⁾ in which a dynamical point of view is introduced. A method of wave packets inside a material is presented, and calculations made for the case of surface plasmons interacting with the Auger electrons. Chase *et al.*⁽¹⁷⁾ have carried out a multibody calculation of the Auger process.

Rather comprehensive calculations on Auger transition rates have been made.⁽¹⁸⁾ Comparison with experimental data is generally satisfactory. In some cases, particularly with transitions involving the outer shells, the results are very sensitive to the choice of wave functions, and consideration of configura-

tion interaction and electron correlation appears to be necessary. For example, Chen and Crasemann⁽¹⁹⁾ have carried out calculations on the *KLL* Auger spectra of elements from $Z = 13$ to 47 using configuration interaction, which substantially improves agreement between experiment and theory.

The selection rules governing Auger transition are that transitions are possible only if the initial and final states have the same symmetries, L , S , J , and parity. Thus, $\Delta L = \Delta S = \Delta J = 0$; $\Pi_i = \Pi_f$. Any three subshells (defined by the principal and angular momentum quantum numbers) can be involved in an Auger process, so long as the difference in total energies between the initial and final states indicates the transition is energetically possible. Table 6.1 lists the relative Auger transition rates for Kr as obtained by experiment and theory. Note the importance of Coster-Kronig transitions.*

We have spoken of the Auger process as being an isolated event involving two and only two electrons. But just as electron shakeoff gives rise to multiple electron ejection in photoionization, this same condition may give rise to two or more electrons being ejected in an Auger process (sometimes called a "double Auger process"). Wolfsberg and Perlman⁽²⁰⁾ were the first to point out that if an Auger electron is ejected from one of the inner shells, an outer shell will experience a sudden change in effective charge and electron shakeoff will occur. The sudden approximation can be invoked to calculate the probability for electron shakeoff (cf. Chapter 3, Section 3.5).

Multiple ionization has also been investigated for Auger processes involving double electron ejection from the valence shell. These studies have been carried out by both charge spectroscopy⁽²¹⁾ and electron spectroscopy.⁽²²⁾ The net change in the effective charge under such circumstances is very small (~ 0.15), yet the probability for double electron ejection runs from 10 to 30 %. Just as with photoionization (cf. Chapter 5, Section 5.1.2.), removal or excitation of more than one electron from the valence shell involves electron correlation, and cannot be explained simply by a net change in electron shielding. A more recent study of this problem has been carried out by Mehlhorn *et al.*⁽²³⁾

Besides the normal Auger process, there also exists what has been called the radiative Auger process or semi-Auger process. In this case there is a simultaneous filling of an inner shell hole and excitation of a second electron with the emission of a single photon. This has been noted⁽²⁴⁾ for *K*-shell x rays in Al, Si, S, and Ar, involving two-electron processes in the $L_{II, III}$ shell. Cooper and

* A Coster-Kronig transition is an Auger transition in which the initial vacancy and one of the electrons that fills this vacancy are in a shell with the same principal quantum number. For example, $L_I - L_{II}M$. Because of the large overlap of the wave functions, Coster-Kronig transitions are more than an order of magnitude larger than normal Auger processes. Whether a Coster-Kronig transition will occur depends on whether the differences in the subshell binding energies are sufficient to eject an electron from an orbital in the next higher shell. For example, the above transition will take place only for elements whose Z is less than 40.

TABLE 6.1
Comparison of Relative Auger Rates in Kr

Transitions	Theory ⁽¹⁸⁾	Experiment
1s 2s 2s	10.3	7.9 ^a
1s 2s 2p	40.0	33.3 ^a
1s 2p 3p	100.0	100.0 ^a
1s 2s 3s	2.9	3.1 ^a
1s 2s 2p	5.3	5.5 ^a
1s 2s 3d } 1s 2p 3s }	5.2	6.3 ^a
1s 2p 3p	26.1	24.7 ^a
1s 2p 3d	3.1	2.6 ^a
1s M M	2.9	—
2s 2p 3p	23.6	—
2s 2p 3d	100.0	—
2s 3s 3s	0.4	—
2s 3s 3p	2.6	—
2s 3s 3d	3.1	—
2s 3p 3p	0.1	—
2s 3p 3d	1.1	—
2s 3d 3d	3.6	—
2p 3s 3s	0.7	—
2p 3s 3p	9.8	—
2p 3s 3s	1.9	—
2p 3p 3p	40.9	22 ^b
2p 3p 3d	68.2	46 ^b
2p 3d 3d	100.0	100.0 ^b
3s 3p 4p	100.0	—
3s 3d 3d	5.8	—
3s 3d 4s	11.3	—
3s 3d 4p	2.9	—
3s 3d 4d	0.7	—
3p 3d 3d	106.5	
3p 3d 4s	21.4	7 ⁽⁴⁰⁾
3p 3d 4p	100.0	100.0 ⁽⁴⁰⁾
3p 4s 4p	0.9	—
3p 4p 4p	2.9	—
3d 4s 4s	11.5	
3d 4s 4p	100.0	100.0 ⁽⁴²⁾
3d 4p 4p	59.4	89.2 ⁽⁴²⁾

^a P. Erman, I. Bergstrom, Y. Y. Chu, and G. T. Emergy, *Nucl. Phys.* **62**, 401 (1965).

^b M. O. Krause, *Phys. Lett.* **19**, 14 (1965); M. O. Krause and T. A. Carlson, *Phys. Rev.* **158**, 18 (1967).

La Villa⁽²⁵⁾ have studied a similar process in potassium chloride, involving a $L_{II, III}$ photon emission and excitation in the valence shell. Here the probability as observed in an x-ray spectrum is as high as 10% of the parent line. Since these processes arise from the emission of a photon and not an electron, they will be experimentally observed in x-ray emission spectra, not Auger spectra.

Finally, we have not discussed the fate of the ion which follows the Auger process. If the Auger process has involved only core electrons, there remain inner shell vacancies that can also be filled by additional Auger processes, creating more ionization. Since each Auger process produces a new vacancy, a series of such processes is called a vacancy cascade. An initial vacancy in a heavy atom will result in a large net charge because of the repetitive Auger processes. For example, Figure 6.2 shows a typical vacancy cascade in Xe. Experimentally, the average charge for xenon following a K vacancy is +8, while ions with charge as high as +22 have been measured⁽²⁷⁾ as the result of a single initial vacancy. Comprehensive studies⁽²⁸⁾ of the net charge resulting

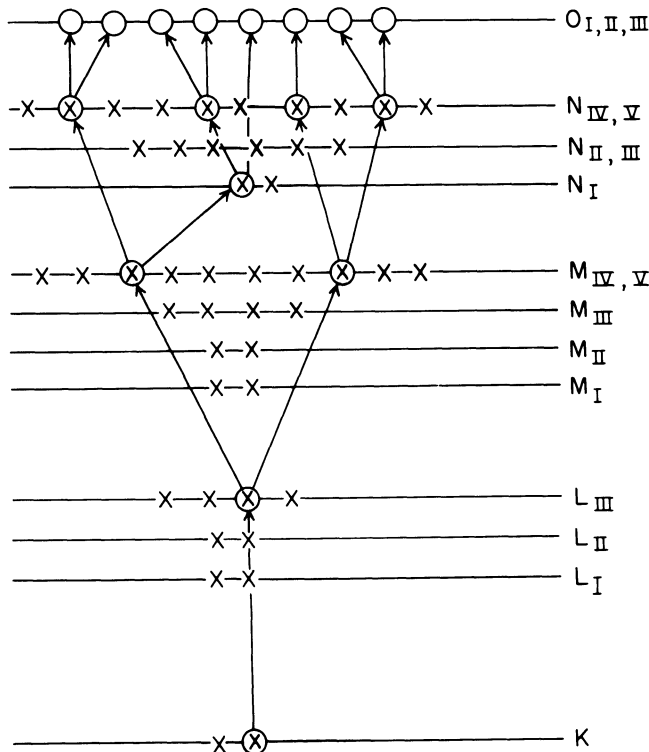


FIGURE 6.2. Schematic representation of a vacancy cascade in Xe. X, Electrons; O, vacancies; \otimes , vacancies that were subsequently filled by electrons.

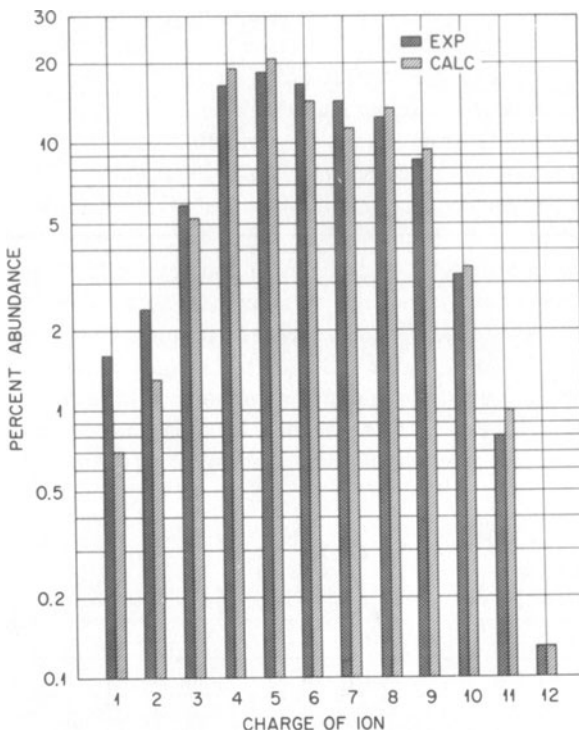


FIGURE 6.3. Experimental charge distribution of Kr ions resulting from irradiation by Mo $K\alpha$ x rays compared with theory. [Reproduced from M. O. Krause and T. A. Carlson, *Phys. Rev.* **158**, 22 (1967), Figure 2.]

from inner shell vacancies have been carried out for both free atoms and molecules. Carlson and Krause⁽²⁹⁾ have shown that observed charge spectra can be accounted for on the assumption that each Auger process acts essentially independently and can be summed by means of a Monte Carlo calculation. To complete the calculation, account is also taken of electron shakeoff. Figure 6.3 shows a comparison between the calculated and measured charge spectrum for Kr following photoionization in the inner shells.

2. COMPARISON OF THE AUGER PHENOMENON WITH THE PHOTOELECTRIC EFFECT AND X-RAY EMISSION

In this section we shall compare the closely related phenomena of the Auger process, photoionization, and x-ray emission. We shall bring together

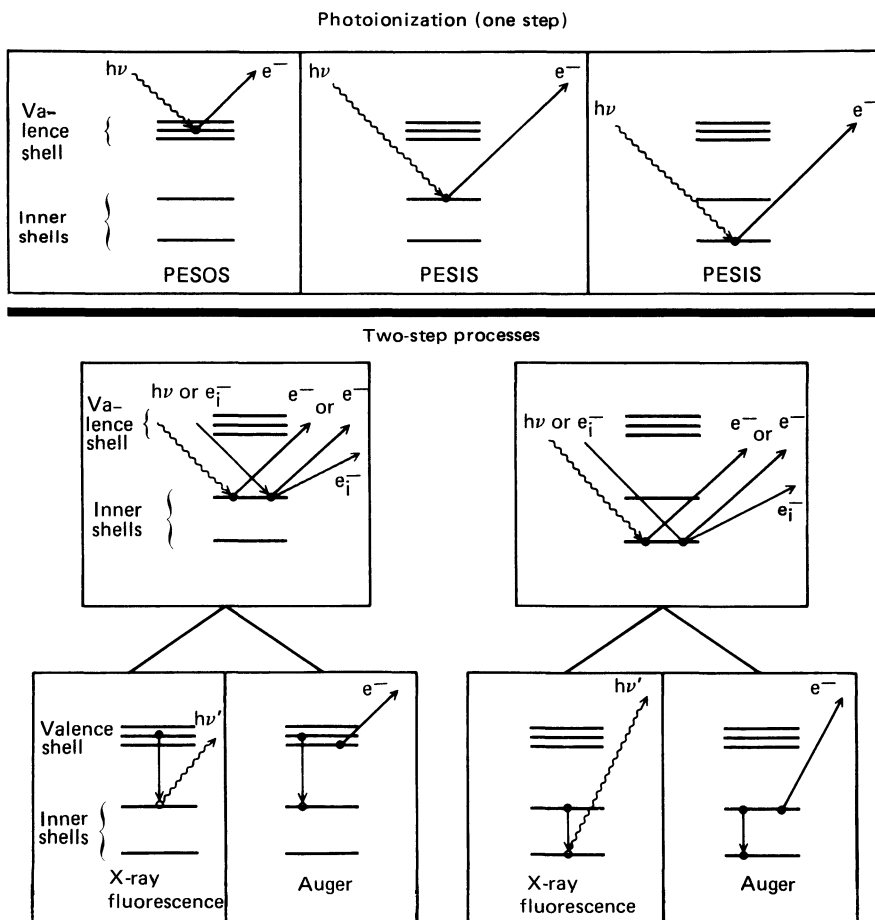


FIGURE 6.4. Basic processes involved in photoelectron, x-ray, and Auger spectroscopy. Comparison of photoelectron, x-ray, and Auger spectroscopy distinguishes between one-step (above) and two-step (below) processes. Photoionization is a one-step process; for both outer shell (PESOS) and inner shell (PESIS) emission we have a simple relation between the measured energy of the emitted electron, the photon energy, and the binding energy in the affected shell. From PESOS we determine valence binding energies of the various molecular orbitals. In PESIS we determine core-electron (atomic) binding energies and note how they vary with chemical environment (chemical shift). X-ray fluorescence and Auger spectroscopy are two-step processes. A photon or an electron ejects an electron from an inner shell. (If we use electrons rather than photons, the incident electron e_i^- is also emitted.) In the second step an electron drops down to fill the hole and either an x ray or a second electron (the Auger electron) is emitted. For x-ray or Auger processes in which an electron drops from a valence shell, the chemical shift tells us about binding energies in both shells. Where the transition is between two inner shells, x-ray spectra are not very useful because the binding energies shift together. Auger spectra should, in principle, be useful for studying inner shell transitions, because the net effect is ejection of an inner shell electron. But complex spectra and short lifetimes limit the usefulness of this type of Auger spectroscopy. [Reproduced from T. A. Carlson, *Physics Today* **25**, 30 (1972), Figure 1.]

material that was touched on before, as well as some new ideas. The task will be completed when we discuss the merits of Auger spectroscopy for studying gases and solids (Sections 3 and 4).

Figure 6.4 illustrates the basic processes. Photoionization is a single-step process involving the ejection of an electron by a photon. Auger and x-ray phenomena are essentially two-step processes. First, an inner shell vacancy is formed, and second, that vacancy is filled either by a radiative or a nonradiative process. The inner shell vacancy can be formed either by electron or x-ray bombardment. If an electron beam is employed, only a portion of the energy of the impact electron is used in the ionization. Both the impact and ejected electrons share the net energy, which equals the difference between the initial and final states of the atom and ion. Thus, unless a coincidence technique is employed, information on atomic and molecular binding energies will not be forthcoming from the continuous-energy electron spectrum formed in the collision process. The cross section for photoejection is usually largest close to the binding energy threshold. The maximum cross section for ionization due to electron impact generally occurs when electron impact energies are several times the binding energy (cf. Figure 6.5 for a typical plot of an electron-impact cross section).

The advantages for using electron impact rather than photons are

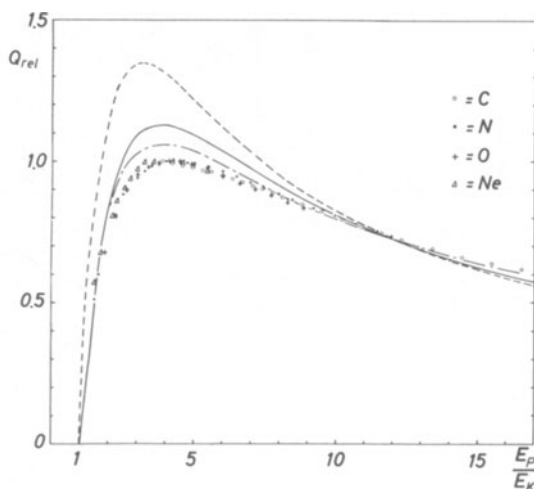


FIGURE 6.5. Relative cross section for K ionization in neon, carbon, nitrogen, and oxygen as function of E_p/E_K , which is the ratio of energy of input electron to K -binding energy. Lines are theoretical predictions. Points are experiment. [Reproduced from Glupe and Mehlhorn,⁽⁵⁶⁾ Figure 1.]

(1) an electron beam can be obtained with many orders of magnitude greater intensity than is possible for an x-ray source, and (2) a well-defined focal spot can be achieved with an electron beam, of inestimable value in surface topography. Although, in principle, soft x rays can be focused, it is impractical with present technology to produce a beam of sharp focus with reasonable intensity. Soft x rays, however, have their advantages for producing inner shell vacancies. In many applications, the intensity of the x-ray beam is more than sufficient. The production of secondary electrons is less, and the peak-to-background ratio is superior to that for electron impact. Less radiation damage is incurred, and the problem of carbon baking is not present. (If a vacuum system is not clean of hydrocarbon vapor from pump oil and O-ring seals, electron bombardment of a surface containing a hydrocarbon film will break down the hydrocarbon and soon a carbon layer will form.) Under less severe radiation the hydrocarbon film will equilibrate on the surface to an amount that is tolerable under many circumstances.

Protons, α -particles, and heavy ions have also been used for promoting inner shell ionization. The chief advantage for using positively charged nuclei rather than electrons occurs in the domain of x-ray emission spectroscopy. Ions do not create the bremsstrahlung background that electrons do. Needham *et al.*⁽³⁰⁾ have used protons in connection with Auger emission to ensure that only surface atoms are excited.

Each of the three methods (photoelectron spectroscopy, Auger spectroscopy, and fluorescence spectroscopy) yields information on binding energies. Photoelectron spectroscopy gives the simplest and most direct information that relates to the binding energy of a single orbital. X-ray emission depends on the binding energy of two shells, while Auger data are the most complex to interpret, depending on the behavior of three shells. For the last two methods the bulk of the transition energy is characterized by an inner shell (the detailed spectrum reflects the nature of the singly and doubly charged final state); thus with all three methods one can determine the binding energy of an inner shell, which in turn affords elemental analysis. This arises because binding energies for the inner shells differ by large amounts, and in most cases are unique to the different elements. The spectra thus obtained by all three of the methods (AES, PES, and x ray) consist of widely separated peaks that provide an easy method of elemental analysis.

The information contained in electron and x-ray spectra concerns the nature of the chemical environment as well as the identification of the element. In comparing the three methods for the sorts of chemical information that can be extracted, we must first recall the differences between the valence and inner shells. The binding energies of the valence shell orbitals are characteristic of the molecule or solid as a whole. With core electrons one is dealing principally with atomic orbitals, which feel changes in chemistry only as a perturbation

in the valence shell potential. Binding energies of the inner shells all change in unison with alterations of the chemical environment. (Cf. Chapter 5, Section 2.)

Let us now turn to each of the three spectroscopic methods to see what chemical information we may gain (cf. Figure 6.4). Photoionization again gives the most direct information by telling us separately either about the valence shell or about the core electron. For Auger or x-ray emissions there are basically two different types of situations. In the first case we have a transition between an inner and an outer shell. The binding energy of the inner shell gives evidence of what element is being investigated. The detailed spectrum depends on the final state of the molecular ion: In the case of x rays it is the singly charged ion, and in the case of Auger processes, the doubly charged ion. The energy spacings in an x-ray spectrum of a given molecule should resemble those found in the direct photoionization spectrum of the outer shell. Which of the states are reached and the intensity of the x-ray peaks corresponding to the states depend on the x-ray transition rates. Until recently, the intensities and resolution of x-ray spectra have not been sufficiently high to make many unambiguous identifications, but technology has advanced to the point⁽³¹⁾ that molecular orbitals can now be clearly identified in x-ray spectra. The study of doubly charged molecular ions by Auger spectra will be discussed in Section 3.

The second situation that can occur for x ray and Auger transitions is to have the transitions occur between two inner shells. Since the chemical shifts for all the core electrons are essentially identical, x-ray energies should be essentially independent of the chemical environment if the radiative transitions occur inside the valence shell. This indeed has been found to be the case. Small shifts are sometimes noted, however. These are due to a breakdown in the assumption that changes in chemical bonding will be felt by the core electrons only in terms of alterations in the outer shell potential. Changes in shielding also occur, as well as changes in the relaxation energies. These are usually minor effects, but can be estimated by observing x-ray spectra. (They can also be estimated by observing the *difference* in chemical shifts between two core shells studied by photoelectron spectroscopy.)

When only core electrons are involved in an Auger process, the net result is the ejection of an inner shell electron. Thus, ejected electrons will feel the potential of the valence shell just as in the case of photoionization, and the chemical shifts observed in Auger spectroscopy of inner shells should be similar to those seen with PESIS. This was first demonstrated by Fahlman *et al.*⁽³²⁾ for the $K-L_{II, III}L_{II, III}$ transitions in sulfur, using $\text{Na}_2\text{S}_2\text{O}_3$. The chemical shift observed in the Auger spectrum between the +6 and -2 oxidation states was 4.7 eV (cf. Figure 6.6). Data from PESIS gave 7.0 eV as the chemical shift between the K shells of the two sulfurs of the $\text{Na}_2\text{S}_2\text{O}_3$ and 6.0 eV for the $2p$ shells.

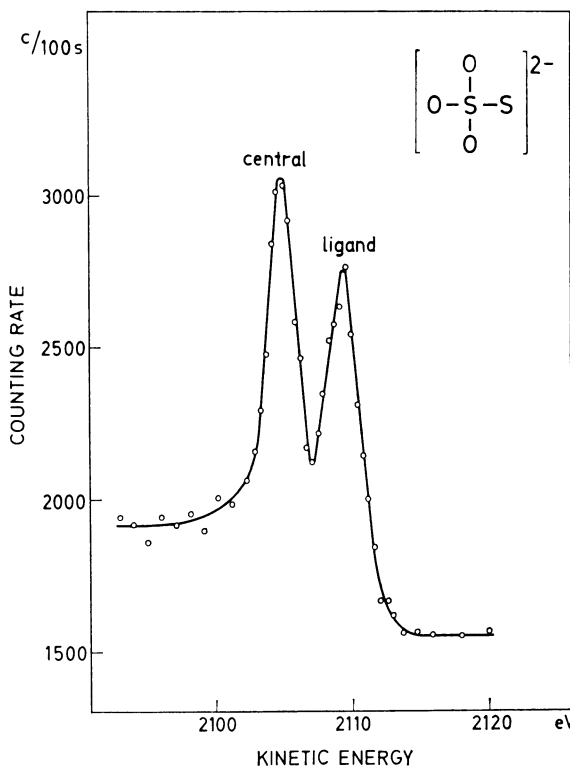


FIGURE 6.6. The $K-LL$ [$2s^22p^4(1D_2)$] Auger spectrum of sulfur for $\text{Na}_2\text{S}_2\text{O}_3$, showing two peaks corresponding to differences in chemical environment. [Reproduced from Fahlman *et al.*⁽³²⁾]

To a good approximation the chemical shift ΔE_A in the Auger transition $K-L_{\text{II, III}}L_{\text{II, III}}$ is

$$\Delta E_A = \Delta E_I - 2 \Delta E(L_{\text{II, III}}) \quad (6.4)$$

Using the data of PESIS, ΔE_A is determined from equation (6.4) to be 5.0 eV, in reasonable agreement with the Auger results. As another example, the KLL Auger spectrum of SiH_4 and SiF_4 were measured.⁽³³⁾ The observed shift was 5.5 eV, in reasonable agreement with the chemical shifts observed in the photoelectron spectra of the $2p$ shells of corresponding silicon compounds. The study of chemical shifts of core electrons by Auger spectroscopy is hampered by the fact that one has to produce a vacancy or principal shell deeper than would be the case of photoionization, with a subsequent broadening in the Auger spectrum due to the larger natural widths of the more deeply lying atomic levels. This broadening, coupled with the more

complex Auger spectra, makes the observation of inner shell chemical shifts more difficult for Auger spectroscopy than for photoelectron spectroscopy.

The simple correlation described above between chemical shifts in photoelectron spectroscopy and Auger spectroscopy does not always occur. Wagner and Biloen⁽³⁴⁾ found, when comparing chemical shifts between some metals and their oxides, that the shifts in the case of Auger processes were much larger (cf. Table 6.2).

This behavior has also been noted by Schön.⁽³⁵⁾ Chemical shifts found from Auger spectra for Na,⁽³⁶⁾ Mg,⁽³⁷⁾ and Al⁽³⁸⁾ and their respective oxides were found to be greater than the chemical shifts seen with PESIS by 5.0, 4.1, and 4.2 eV, respectively. Wagner and Biloen have attributed these differences to the higher polarization afforded the case of an Auger process where there are two core vacancies in the final states, which is to say the extraatomic relaxation effect. In photoionization we have the difference between a neutral species and the relaxation given by a single hole. In the Auger process we begin with a single relaxed hole and end with a double vacancy which requires relaxation. The effects are most apparent when comparing metals and dielectrics, but slight differences were also found between different sodium and zinc compounds.⁽³⁶⁾ Since Auger and XPS measurements can be made on the same material at the same time, relative shifts from compound to compound might be a valuable method for appraising extraatomic relaxation effects.

Knowledge of the chemical environment can be obtained most directly and easily by photoelectron spectroscopy, but Auger electron spectroscopy and x-ray emission spectroscopy may also be used in the study of chemical bonding. Information from all three methods supplements one another.

For our final comparison of the three spectroscopies, let us turn to the subject of surfaces. The surface depth that is studied depends on penetration

TABLE 6.2
Chemical Shifts between Element and Oxide for Selected Auger and Photoelectron Lines^a

Element	Photoline shifts, eV			Auger line shifts, eV	
	$2p_{3/2}$	$3d_{5/2}$	$4d$	<i>LMM</i>	<i>MNN</i>
Zn	0.4	0.6	—	4.2	—
Ga	1.7	2.2	—	6.2	—
Ge	3.0	3.3	—	6.7	—
As	2.3	3.6	—	6.4	—
Cd	—	0.4	0.9	—	5.5
In	—	0.8	0.9	—	2.6
Sn	—	1.5	1.2	—	3.9

^a Taken from Wagner,⁽³⁴⁾ Table 3.

TABLE 6.3
**Comparison of Average Auger and
 Photoelectron Energies for the First Row
 Elements**

Element	<i>K</i> - <i>LL</i> Auger, ^a eV	<i>E_e</i> , ^b eV
Li	45	1199
Be	100	1143
B	176	1066
C	266	970
N	375	855
O	507	732
F	654	568
Ne	813	387

^a Position of most intense peak. C to Ne from Siegbahn *et al.*⁽⁴²⁾; Li to B from Palmberg *et al.*⁽¹⁵⁾

^b Photoelectron energy using Mg *K* α x rays.

of the excitation source and the probability for escape of the electron or x ray being measured. From Figure 5.42 it is evident that the mean free path for photons is always several orders of magnitude larger than for electrons of the same energy. We may thus conclude that the escape depth is determined entirely by kinetic energy of the electrons involved. Table 6.3 shows the photoelectron and Auger energies expected for the first row elements. Comprehensive tables⁽⁹⁾ and graphs⁽¹⁵⁾ of the approximate photoelectron energies and Auger energies normally encountered in electron spectroscopy are available. For heavier elements the Auger and photoelectron energies are more varied. In both instances the energies will vary from about 100 to 1500 eV. When comparing Auger electrons with photoelectrons formed by irradiating with Mg *K* α x rays, the Auger electrons are usually found to be lower in energy, but sometimes the reverse is true. In addition, lower photon energies can be employed, such as Y and Zr *M* ζ lines (132.3 and 151.4 eV), which will produce correspondingly lower photoelectron energies. Thus, Auger and photoelectron spectroscopy examine essentially the same region of surface. This is certainly true if x rays are employed as the initial excitation source. If electron impact is employed, the depth for forming the initial vacancy is reduced. But in producing the initial vacancy, the energy of the impact electron is generally chosen to be at least several times that of the subsequent Auger electron. Thus, it is still the mean free paths of the escaping Auger electrons that essentially determine the depth of the surface layer measured. When x rays produced by fluorescence are measured, the depth of the surface being studied increases substantially. If photoionization is employed as the initial excitation source, the measurements are made well into the bulk material. If electron impact is used, we must re-

TABLE 6.4
Approximate Surface Depth Studied as a Function of Analysis^a

Excitation	Emission	Surface thickness, Å
e ⁻	Auger electron	20
X ray	Photoelectron	20
X ray	Auger electron	20
e ⁻	X ray	600 ^b
X ray	X ray	40,000

^a Based on mean free path of electrons and x rays in Al, assuming 1-keV ejected electron or x ray, 1.5-keV impact x ray, and 10-keV impact electron.

^b Mean free path for core ionization taken as five times larger than plasmon loss.

member that one is concerned with the distance an electron can travel while still maintaining sufficient energy for inner shell ionization. This is considerably larger than just the mean free path for electrons undergoing inelastic scattering, which is of importance if we wish to detect a discrete energy electron. It has been estimated,⁽³⁹⁾ in fact, to be approximately five times the mean free path. Table 6.4 summarizes the above discussion by giving a rough idea of the surface depth measured by the various methods. Considerable variations are possible (cf. Section 3 for further discussion of surface problems).

3. USE OF AUGER SPECTROSCOPY FOR GASES

The high resolution possible for measuring electrons ejected from a gas target and the simplifying conditions encountered when dealing with individual molecules or ions have made the study of the Auger spectra of gases a fruitful area for fundamental research. Details of the Auger process itself, the nature of the ground and excited states of the doubly charged ions, and the various phenomena associated with the initial excitation processes are topics that will be discussed in this section. In addition, we shall try to evaluate the potential for gas analysis by Auger spectroscopy.

3.1. Atoms

Mehlhorn^(40, 41) was the first to demonstrate the advantages of studying the Auger spectra of gaseous atoms with high resolution. These studies gave fine details against which the concepts of the Auger process could be tested. Subsequently, extensive data on the rare gases were obtained by the group at

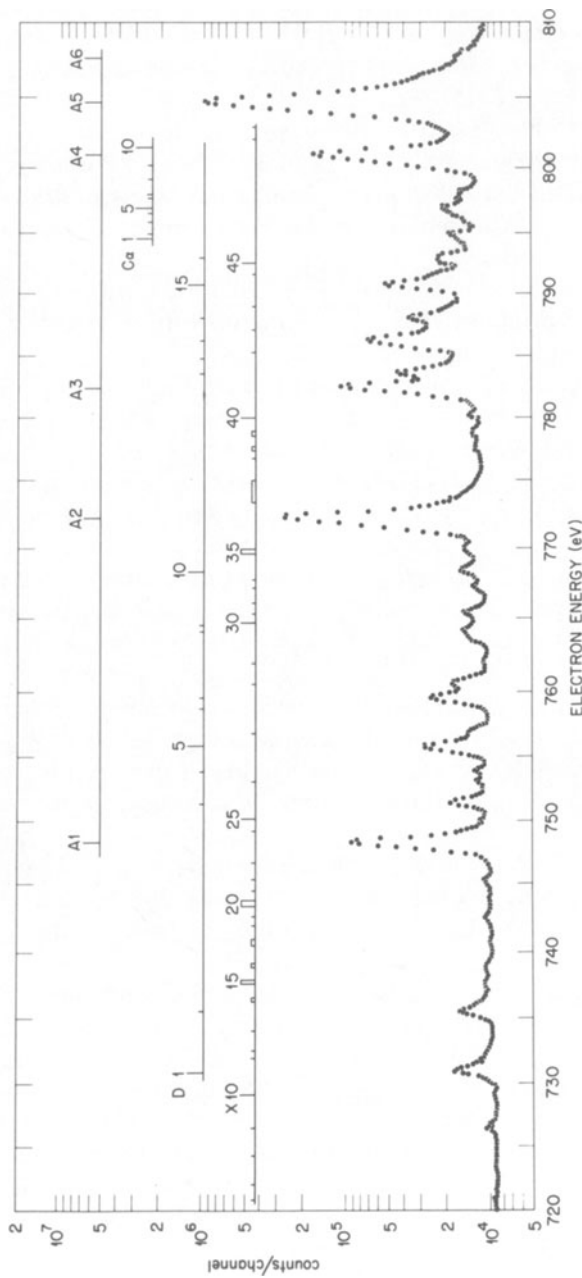


FIGURE 6.7. Neon K Auger spectrum excited by 4.5-keV electrons. The A lines are diagram Auger lines; the $C\alpha$ lines are shakeup processes, and the D lines are from electron shakeoff. [Reproduced from Krause *et al.*, (44) Figure 1.]

Uppsala^(42, 43) and by Krause *et al.*⁽⁴⁴⁾ Sodium has also been studied by Hillig *et al.*⁽⁴⁵⁾ Auger spectra arising from filling the *M* and *L* shells as well as the *K* shell were taken, and even the low-energy spectra due to Coster-Kronig transitions have been recorded.⁽⁴⁰⁾

Flügge *et al.*⁽⁴⁶⁾ have measured the angular distribution of ejected Auger electrons. They have demonstrated that a nonisotopic distribution relative to a directed unpolarized electron or photon beam is possible if an electron with a quantum number $j > 1/2$ is removed and if the resulting atomic state has a quantum number $J'' > 1/2$.

In addition to the normal Auger lines, whose energy spacings can be accurately checked by optical data, a wealth of other lines (satellite lines) are observed. An idea of the complexity of a well-resolved Auger spectrum is given by Figure 6.7. To give some understanding of where these lines arise and of the type of phenomena on which they shed light, let us review the paper by Krause *et al.*⁽⁴⁴⁾ on the *K-LL* Auger spectrum of neon.

Some 90 lines were observed. Of these only five were the normal *K-LL* Auger lines expected from pure Russel-Saunders coupling. A sixth line due to the forbidden $K-L_{III}L_{III}$ 3P transition was found with an intensity of 0.05% of the most intense line. The normal *K-LL* lines arise from transitions in which a single vacancy appears in the *K* shell for the initial state and two vacancies in the *L* shell occur for the final states; otherwise, the other electrons are in the same configuration as they would be for a neon atom. A satellite line occurs when the configuration is altered from that described above, either for the initial or the final state. Figure 6.8 illustrates the various types of processes that lead to satellite lines. Though the normal lines make up the majority of the Auger spectra, the contribution from satellite lines is by no means negligible.

As mentioned before, the nomenclature for describing an Auger process is to designate the shells in which the vacancies occur. In addition, we use the letter *e* to designate a single electron which has been placed into an excited state.

Let us briefly discuss the nature of these satellite processes. First, a *K* vacancy can be formed without having the electron originally in the *K* shell go into the continuum, but rather having it promoted into an excited but bound neutral state. This may occur with photons whose energy exactly matches the transition to the highly excited *K*-hole state, whereupon resonance absorption occurs. When monochromatic x rays are used whose energies are in excess of the *K* binding energy, such resonance absorption cannot occur; but impact electrons utilize only a portion of its energy and can easily form *K*-hole excited states. From the analysis of the neon Auger spectrum it was ascertained that when a *K* vacancy was created by electron impact it took place by excitation in

DESIGNATION	DESCRIPTION	INITIAL CONFIGURATION	FINAL CONFIGURATION	CHARGE OF ION
K-WW	NORMAL	W ——— S ———	W —○—○ S ———	2
		K —○—	K ———	
—	—	—	—	—
K-WS	NORMAL	W ——— S ———	W —○— S —○—	2
		K —○—	K ———	
—	—	—	—	—
K-SS	NORMAL	W ——— S ———	W ——— S —○—○	2
		K —○—	K ———	
—	—	—	—	—
Ke-W	EXCITATION OF K SHELL ELECTRON INTO DISCRETE STATE, FOLLOWED BY DECAY INVOLVING EXCITED ELECTRON	e -----x--- W ——— S ———	W —○— S ———	1
		K —○—	K ———	
—	—	—	—	—
Ke-WW	EXCITATION OF K SHELL ELECTRON INTO DISCRETE STATE, NOT INVOLVING EXCITED ELECTRON	e -----x--- W ——— S ———	W —○—○ S ———	1
		K —○—	K ———	
—	—	—	—	—
Kwe-WW	MONPOLE EXCITATION FOLLOWED BY DECAY INVOLVING EXCITED ELECTRON	e -----x--- W —○— S ———	W —○—○ S ———	2
		K —○—	K ———	
—	—	—	—	—
Kwe-www	MONPOLE EXCITATION FOLLOWED BY DECAY NOT INVOLVING EXCITED ELECTRON	e -----x--- W —○— S ———	W —○—○—○ S ———	2
		K —○—	K ———	
—	—	—	—	—
KW-www	MONPOLE IONIZATION	W —○— S ———	W —○—○—○ S ———	3
		K —○—	K ———	
—	—	—	—	—
K-www	DOUBLE AUGER IONIZATION	W ——— S ———	W —○—○—○ S ———	3
		K —○—	K ———	

FIGURE 6.8. Designation for the various types of Auger processes observed in a $K-L_L$ Auger spectrum where the L shell is the valence shell of the atom. W and S designate orbitals in the valence shell in which the electrons are, respectively, relatively weakly or strongly bound. For the case of a free atom $W = L_{2,3}; S = L_1$. An excited orbital is designated e . [Reproduced from Moddeman *et al.*,⁽⁴⁸⁾ Figure 1.]

about 2% of the time and by ionization for the remainder. This ratio remains approximately the same over the energy range of the incident electrons from 2 to 6 keV. It was further ascertained that the excitation took place preferentially to the np states rather than ns states, indicative of a dipole transition.

Following K -shell excitation the vacancy may be filled by either radiative or nonradiative transitions. If a nonradiative transition occurs, discrete-energy electrons are ejected, as in the normal Auger processes, although the final state is a singly charged ion. Two possible spectra arise according to whether (1) the electron placed into the excited state acts as a spectator while an Auger process takes place with two of the more tightly bound electrons, or (2) the electron in the excited state is directly involved in the filling of the K hole. Both cases result in electron energies that are higher than the normal Auger lines, with case 2 having the higher energy. Substantial data have been taken on satellite Auger lines arising from excited K holes for simple molecules, and further details will be discussed in the next section.

Monopole excitation and ionization, or, as they are usually called, electron shakeup and shakeoff, occur as the result of an inner shell vacancy, caused either by photoionization or electron impact. These phenomena have been discussed previously in some detail (cf. Chapters 3 and 5). If electron shakeoff occurs, the final state of the ion following the Auger process will be +3. These satellite lines appear at energies generally lower than the normal Auger lines. (When we say that the satellite lines fall at energies higher or lower than the normal lines, we imply a relationship between the lines of both series. The complete spectrum extends over 169 V, with the different spectra overlapping with one another.) If monopole excitation or electron shakeup occurs, an electron is placed in an excited state, and it either may behave as a spectator or be directly involved in the Auger process. It is much more probable that the electron behaves as a spectator, because there are more electrons in the filled L shell and because this shell has a greater overlap with the $1s$ shell than does the excited orbital. The Auger energies corresponding to the $KLe-LLe$ processes are slight lower and those to the $KLe-LLL$ processes slightly higher than those for the corresponding normal Auger processes.

Satellite lines occur corresponding to the excitation or ionization of an additional electron accompanying the normal Auger process, that is to say, the double Auger process. Since these processes always require extra energy, the Auger electrons are ejected with energies below those of the corresponding normal Auger processes. In the case of double ionization the two electrons share the energy, and the result is a continuum spectrum. Just as in the case when double electron ejection occurs in photoionization, one of the electrons carries away the bulk of the energy.

3.2. Molecules

The first high-resolution Auger spectra in molecules were taken by Stalherm *et al.*⁽⁴⁷⁾ A number of studies have since been carried out at Uppsala⁽⁴²⁾ and at Oak Ridge.⁽⁴⁸⁾ The Auger spectra of molecules are considerably more complex than the corresponding spectra for atoms. This is due in part to the larger number of molecular orbitals and in part to the added complexity of vibrational structure.

As was mentioned earlier, Auger transitions between only inner shells give chemical shifts that are similar to those observed with photoionization. More extensively studied and more interesting because of the unique information that is available are the *K*-*LL* Auger transitions in which the *L* shell is the valence shell, which is to say Auger transitions occurring for the first row elements, including boron, carbon, nitrogen, oxygen, and fluorine. Our attention will be concentrated on Auger spectra involving these elements.

Moddeman *et al.*⁽⁴⁸⁾ have provided a generalized scheme for analyzing the various portions of the *K*-*LL* Auger spectra of molecules. It consists in (1) determining which portions are due to normal Auger processes and which are satellite peaks; (2) dividing the normal Auger lines into categories as to whether they are derived from molecular orbitals whose electrons are weakly or strongly bound; and (3) identifying specific Auger peaks with the help of theory or optical data. Let us describe in turn each of these different parts of the analysis.

First, one needs to identify the satellite peaks. The basic origin of these extra Auger peaks has been discussed in Section 3.1 on atoms. The most important portion of the spectrum to clarify is the high-energy end. This portion is entirely made up of satellite lines. (In the analysis it is given the letter *A*, while the normal lines are divided into portions *B*, *C*, and *D*. For example, see Figure 6.9, showing the Auger spectrum for N₂.) The key to analyzing an Auger spectrum is to find the highest energy peak due to a normal Auger process, since this peak, if observable, should correspond to the lowest energy or ground state of the doubly charged molecular ions. Often this identification is aided by the fact that the transition to the ground state is also one of the most intense transitions. For an example of how high-energy peaks can be properly identified as satellite peaks or normal Auger lines, let us examine the case of nitrogen in Figure 6.9. Peaks *A*-1 and *A*-2 are believed to be due to *K*-hole excitation followed by an Auger process in which the excited electrons directly participate (i.e., *Ke*-*LL*). This is verified by observing that

$$E_A = E^*(K) - E_B \quad (6.5)$$

where E_A is the measured energy for the Auger peaks *A*-1 and *A*-2, $E^*(K)$ is the energy required to place the *K* electron into the first excited state, which has been measured by Nakamura *et al.*⁽⁴⁹⁾ for resonance absorption states to be

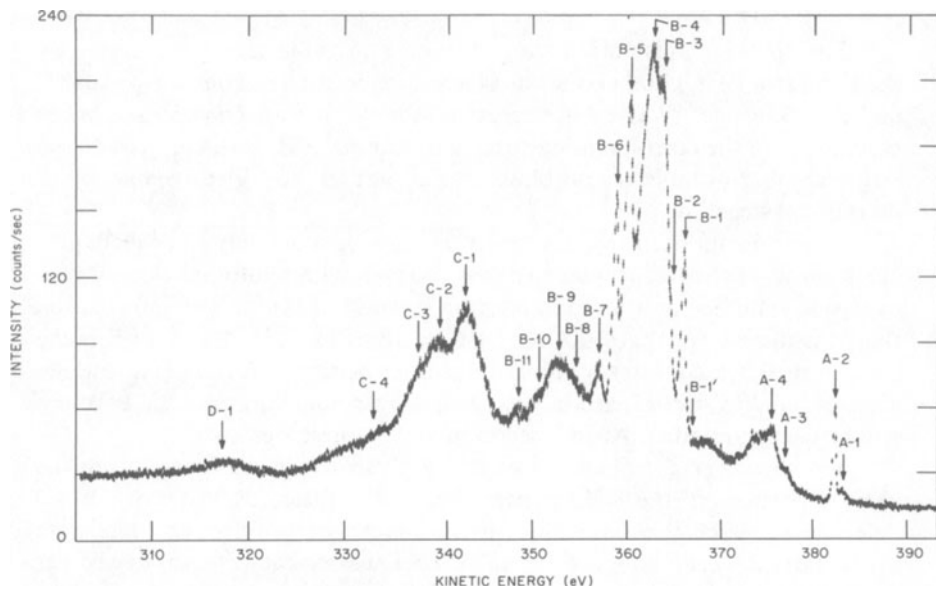


FIGURE 6.9 The $K-LL$ Auger spectrum of N_2 excited by electron impact. See Table 6.5 for identification of labeled peaks. [Reproduced from Muddeman *et al.*,⁽⁴⁸⁾ Figure 2.]

400.2 eV, and E_B is the binding energy for the two least bound orbitals of N_2 . From equation (6.5) one obtains 384.6 and 383.5 eV for E_A , in excellent agreement with the energy of the Auger lines $A-1$ and $A-2$. In addition, it is expected that satellite lines due to $K-LL$ excitation will disappear when $Al\text{ }K\alpha$ x rays are used rather than electron impact to create K vacancies. (The 1487-eV photons will only cause ionization and not excitation of the K -shell electrons.) Indeed, the $A-1$ and $A-2$ peaks are missing in the Auger spectrum of N_2 generated by $Al\text{ }K\alpha$ x rays. Other portions of the spectrum are also missing. (The shaded area in Figure 6.10 represents the difference in the Auger spectra of N_2 as produced by electron impact and by $Al\text{ }K\alpha$ x rays.) These portions are believed due to transitions where the excited electron remains as a spectator (i.e., $Ke-LLe$). In addition, another part of the spectrum in region A is believed to be due to electron breakup (i.e., $KLe-LL$). The energy of these satellite lines is greater than that of the corresponding normal Auger line ($K-LL$) by just the amount involved in electron breakup. The breakup energies in turn have been determined by photoelectron spectroscopy.⁽⁵⁰⁾ In Figure 6.10 the dashed lines give the normal Auger spectrum shifted by the energy of monopole excitation. The relative intensities are, however, strongly dependent on the relative transition rates and will not necessarily be the same as the normal Auger spectrum.

Assignments for the high-energy satellite Auger lines having been made, the peak *B*-1 is said to be first normal line, which is confirmed by good agreement with the appearance potential for N_2^{2+} , using mass spectrometry. Before giving specific designations to the individual peaks, let us next consider the overall breakdown of the normal Auger spectrum. To accomplish this breakdown, we shall divide the orbitals that make up the *L* valence shell into *W* and *S* orbitals, which are so designated because the electrons in these orbitals are either weakly or strongly bound. Thus, the normal Auger processes *K*-*LL* will be now subdivided into *K*-*WW*, *K*-*WS*, and *K*-*SS*, and the energy regions to which they correspond will be called *B*, *C*, and *D*, respectively. Our job will next be to calculate at what energy these processes will occur. This can be done by relating the differences in energy to the various ways of removing two electrons from a neutral molecule. Consider an atom or molecule with shells 1, 2, . . . , where 1 represents the least tightly bound orbital, 2 the next least tightly bound, etc. If coupling in the final states of the doubly charged ion is

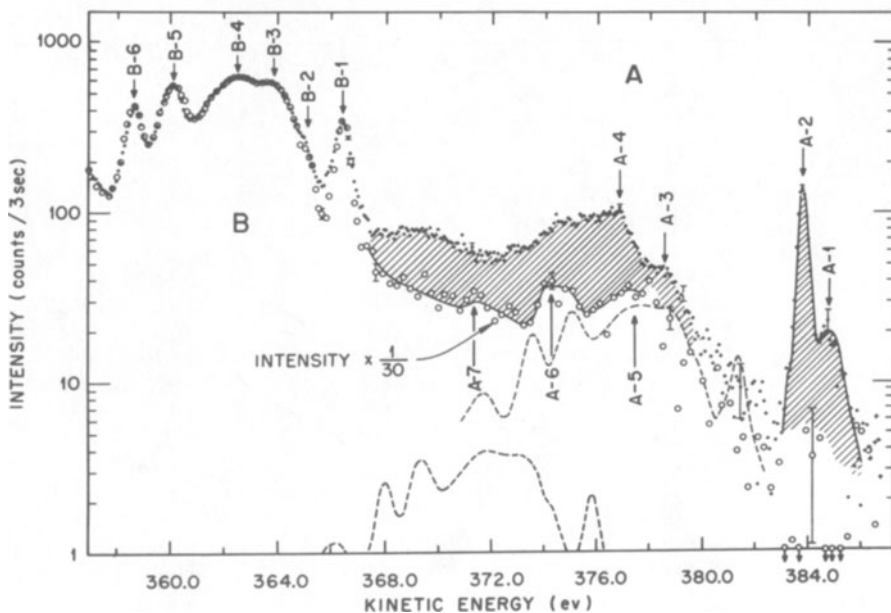


FIGURE 6.10. High energy portion of the *K*-*LL* Auger spectrum of molecular nitrogen excited by electrons and $\text{Al K}\alpha$ x rays. (+) Data from electron impact; (○) data from x-ray bombardment. Shaded area gives the difference between two experiments. Dashed lines give approximate expected shape due to *KWe*-*WWW* processes. [Reproduced from Moddeman *et al.*,⁽⁴⁸⁾ Figure 3.]

ignored, the relative energy of the Auger lines resulting from vacancies in the first two orbitals may be taken as

$$E_A(1) - E_A(2) = \varepsilon_2 - \varepsilon_1 \quad (6.6)$$

$$E_A(1) - E_A(2) = 2(\varepsilon_2 - \varepsilon_1) - C(\varepsilon_1 - \varepsilon_2) \quad (6.7)$$

$E_A(1)$, $E_A(2)$, and $E_A(3)$ are the Auger lines or bands, with $E_A(1)$ representing the highest kinetic energy process, $E_A(2)$ the next, etc.; ε_n is the binding energy of orbital n ; and C is a factor which is related to change in the configuration as electrons are successively removed. C may be obtained empirically or from a simple model. It was found that for both atoms and molecules C is approximately 0.1 $K-LL$ Auger processes. In any case it is not a sensitive parameter.

TABLE 6.5
Assignment of Peaks Appearing in the $K-LL$ Auger Spectrum of N_2^a

Line	Energy, ^b eV	Transition ^c	Initial state		Final state		Calc. E , eV
			q	Desig.	q	Desig.	
A-1	384.7 (4)	$Ke-2p\sigma_g$	0	$(1s)^3(2p\pi_g)^1$	1	$X^2\Sigma_g^+$	384.6
A-2	383.8 (2)	$Ke-2p\pi_u$	0	$(1s)^3(2p\pi_g)^1$	1	$A^2\Pi_u$	383.5
A-3	378.6 (5)	$Ke-WWe$	0	$(1s)^3(2p\pi_g)^1$	1	—	—
A-4	376.7 (6)	$Ke-WWe$	0	$(1s)^3(2p\pi_g)^1$	1	—	—
A-5	378.3 (5)	$KWe-WW$	1	—	2	—	—
A-6	375.0 (5)	$KWe-WW$	1	—	2	—	—
A-7	371.7 (6)	$KWe-WW$	1	—	2	—	—
B-1'	367.0	$K-WW$	1	$(1s)^3$	2	—	367.2
B-1	366.5 (2)	$K-2p\sigma_g 2p\sigma_g$	1	$(1s)^3$	2	$X^1\Sigma_g^+$	—
B-2	365.0 (4)	$K-WW$	1	$(1s)^3$	2	$b^1\Pi_u$	365.2
B-3	363.5 (5)	$K-WW$	1	$(1s)^3$	2	$A''^3\Sigma_u^+$	364.0
B-4	362.5 (5)	$K-WW$	1	$(1s)^3$	2	$A^3\Pi_g$	363.0
B-5	360.2 (2)	$K-WW$	1	$(1s)^3$	2	$c^1\Pi_g$	360.6
B-6	358.7 (2)	$K-WW$	1	$(1s)^3$	2	$d^1\Sigma_u^+$	358.6
B-7	356.9 (3)	$K-WW$	1	$(1s)^3$	2	$e^1\Sigma_g^+$	356.7
B-8	354.7 (6)	$KW-WWW$	2	—	3	—	—
B-9	352.5 (6)	$KW-WWW$	2	—	3	—	—
B-10	350.4 (6)	$KW-WWW$	2	—	3	—	—
B-11	347.8 (6)	$KW-WWW$	2	—	3	—	—
C-1	342.4 (4)	$K-WS$	1	$(1s)^3$	2	—	—
C-2	339.1 (5)	$K-WS$	1	$(1s)^3$	2	—	—
C-3	337.4 (6)	$K-WS$	1	$(1s)^3$	2	—	—
C-4	332.7 (7)	—	—	—	—	—	—
D-1	315.0 (9)	$K-2s\sigma_g 2s\sigma_g$	1	$(1s)^3$	2	$^1\Sigma_g^+$	—

^a Taken from Moddeman *et al.*,⁽⁴⁸⁾ Table 2.

^b Uncertainty in energy given for last significant figure in parentheses.

^c Compare with Figure 6.8 for description of terms. Specific designations of orbitals are given rather than *W* or *S* when they are known with some degree of confidence.

In order to apply equation (6.7) for estimating the relative energies represented by regions *B*, *C*, and *D*, ε_2 is generally taken to be the more tightly bound $2s\sigma$ orbital, while ε_1 is an average of the remaining less tightly bound orbitals. In general, regions *C* and *D* were found to be respectively about 20 and 40 V lower than region *B* (cf. Figure 6.9 for nitrogen).

Returning to the analysis of some of the specific peaks of the Auger spectrum, it should be remembered that the energies of the different lines arising from normal Auger processes are related to one another by the energy separation between the various excited states of the doubly charged molecular ions. The most important peak is designated *B*-1 and represents an Auger transition to the ground state. The energy differences between this line and the lower energy normal Auger line are the excitation energies for the doubly charged ions. In the case of nitrogen it has been possible to assign states to some of the Auger lines by using the energy differences of the isolated curves of N_2^{2+} as derived by Hurley.⁽⁵¹⁾ The analysis of the *K*-*LL* Auger spectrum of nitrogen is given in Table 6.5. Similar analyses have been made for O_2 , CO, NO, H_2O , and CO_2 .

From the highest-energy normal Auger line designated *B*-1 one can obtain the minimum energy for double electron removal $E_{II}(\text{min})$ from the relationship

$$E_{II}(\text{min}) = E(K) - E_A(B-1) \quad (6.8)$$

where $E(K)$ is the binding energy of the *K* shell and $E_A(B-1)$ is the measured Auger energy for the highest-energy normal Auger lines. (To be more accurate, the onset of this line (*B*-1') is usually used, which ought to correspond more closely to the adiabatic ionization potential) Table 6.6 lists $E_{II}(\text{min})$ for a number of molecules using Auger spectroscopy together with appearance potentials

TABLE 6.6
Minimum Energy Required for Producing Doubly and
Triply Charged Molecular Ions

Ion	$E(\text{min})$, eV	
	Auger spectra ⁽⁴⁸⁾	Electron impact ^a
$(N_2)^{2+}$	42.9	42.7
$(N_2)^{3+}$	84	—
$(O_2)^{2+}$	37.4	36.5
$(CO)^{2+}$	39.9 (C), 40.2 (O)	41.8
$(NO)^{2+}$	35.7, 40.1 (N) 34.7 (O)	39.8
$(H_2O)^{2+}$	39.2	—
$(CO_2)^{2+}$	37.8 (C), 37.4 (O)	36.4

^a J. L. Franklin *et al.*, *Natl. Std. Ref. Data Ser., Natl. Bur. Std.* 26 (1969).

as obtained from mass spectroscopy. In one case, nitrogen, it was also possible from Auger data to estimate the energy necessary to form the triply charged ion. In general, the agreement between values arrived at by Auger spectroscopy and those obtained by mass spectroscopy is good. Auger spectroscopy has a distinct advantage over mass spectroscopy in determining the minimum energy for forming molecular ions, since in mass spectroscopy the ion must remain intact the 10^{-5} sec required to detect it, while meaningful results can be obtained from Auger spectra without the requirement that the ion remain stable.

Besides the formal methods for analyzing molecular Auger spectra that have been discussed in the preceding paragraph, there are several other observations that can be of assistance. First, it is of value to compare the Auger spectra corresponding to different elements of the same molecule. The energy spacings in both spectra correspond to those that are expected for the various states of the doubly charged molecular ion that is the result of a K -LL Auger process. The total Auger energy depends on the element in which the initial K vacancy is formed, but the energy spacing depends primarily on the states of the doubly charged molecular ion. The probability for reaching a given state will depend on whether the orbitals involved in the transition are strongly associated with the atom having the K vacancy. For example, Figure 6.11, compare the Auger spectrum corresponding to K vacancies in carbon and in oxygen of CO. The peaks are labeled identically when it is felt that they both represent the same final state. Neumann and Moskowitz⁽⁵²⁾ have calculated the atomic population of the molecular orbitals of CO and find the percentage carbon character in each orbital to be as follows: $2p\sigma^b$, 92%; $2p\pi^b$, 33%; $2s\sigma^*$, 20%; and $2s\sigma^b$, 33%. (For example, one would expect that Auger processes filling a vacancy in the K shell of carbon would involve the $2p\sigma^b$ orbitals much more readily than would be the case if the K vacancy occurred with oxygen.) This information helps us in assigning the origin of the various Auger peaks. Thus, the presence of the strong peaks B -1, B -2, and B -3 found in the carbon spectrum, which are weak or missing in the oxygen spectrum, suggests these peaks involve $2p\sigma^b$ orbitals. The strongest peaks for the oxygen spectrum of CO occur between B -5 and B -7 and apparently involve the $2p\pi^b$ and $2s\sigma^*$ molecular orbitals. These suggestions are further supported by the fact that the binding energy of the $2p\sigma^b$ orbital is less than that of the $2p\pi^b$ and $2s\sigma^*$.

Another source of information for analyzing the Auger spectrum comes from vibrational structure. Normally such structure is not readily seen because of the complexity of the Auger spectra and the need for very high resolution. However, it has been observed in the carbon spectrum of CO (cf. details of high-energy portion of carbon Auger spectrum of CO, Figure 6.12). These three bands are believed to arise from a K -vacancy excitation in which the excited electron participates in the subsequent reorganization, i.e., $Ke-L$. The final

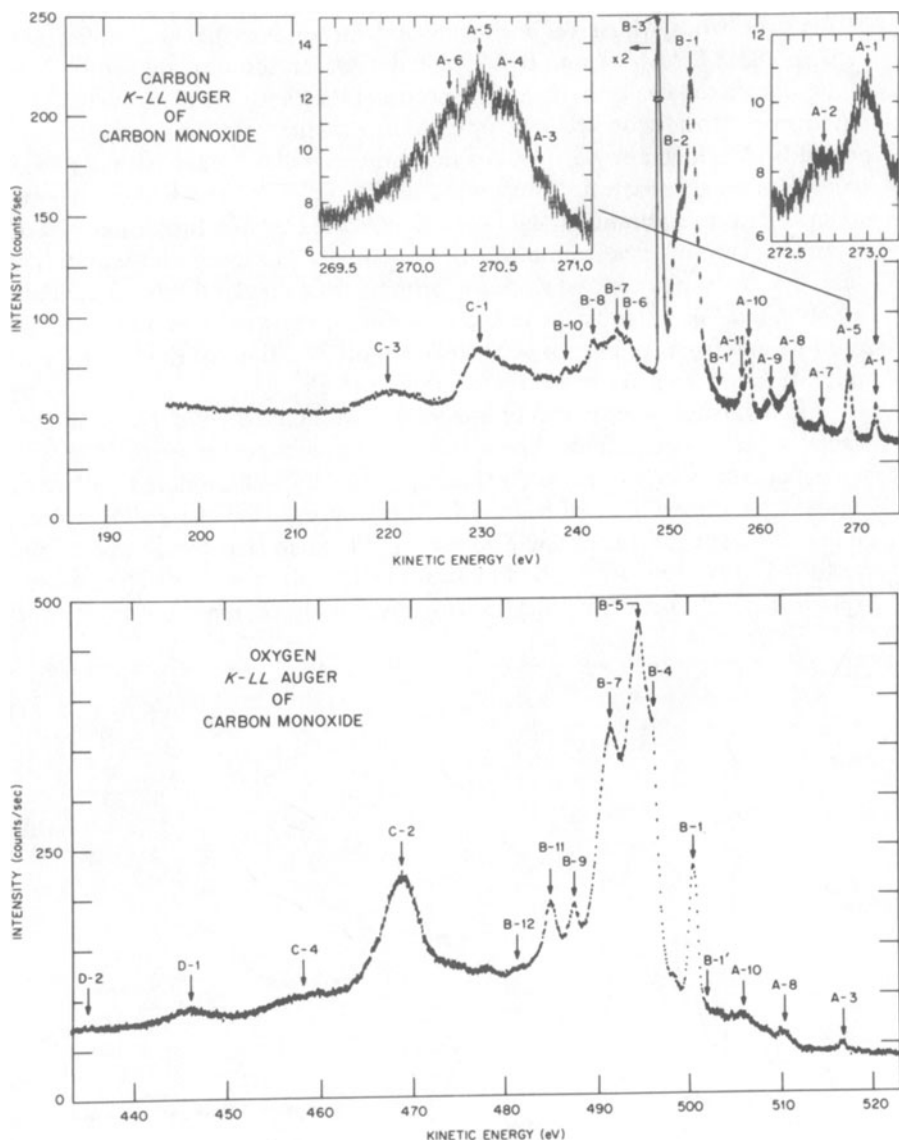


FIGURE 6.11. Comparison of the K - LL Auger spectra in CO resulting from K vacancies in C and O, respectively. Peaks labeled the same are believed to belong to the same final state of the molecular ion. [Reproduced from Moddeman *et al.*,⁽⁴⁸⁾ Figures 6 and 7.]

state is the singly charged carbon monoxide and the bands resemble the photo-electron spectrum of the same molecule with regard to the energy separation between the bands, which is equivalent in both instances to the energy difference between the $X^2\Sigma^+$, $A^2\Pi$, and $B^2\Sigma^+$ states of CO^+ . In addition, the separations of the vibrational peaks in the Auger spectra of the bands are identical to those found in photoelectron spectroscopy. Some evidence of a hot band was reported by Moddeman *et al.*⁽⁴⁸⁾ but the more significant fact is that it was small. Hot bands arise when the vibrational states of the initial molecule are excited. Thus the vibrational data on CO indicate that the formation of a K vacancy in carbon leaves the molecules essentially in the ground vibrational state. This is to be expected since the orbitals which make up the K shell are nonbonding. Also significant is the fact that vibrational structures can be resolved, and from the line shape Siegbahn *et al.*⁽⁴²⁾ estimated that the natural width of Auger lines for carbon is less than 0.18 eV.

Finally, Auger spectra can be analyzed by comparison of data in a homologous series of compounds. Spohr *et al.*⁽⁵³⁾ have studied a series of brominated methanes and Moddeman⁽³³⁾ has reported data on fluorinated methanes. Figure 6.13 shows the carbon K - LL Auger spectra for the hydrocarbons methane, ethane, and benzene. Spohr *et al.*⁽⁵³⁾ noted that the sharpest lines are found in benzene while the broadest are seen for methane. The authors explain this in terms of the lifetimes for the doubly charged molecules. The

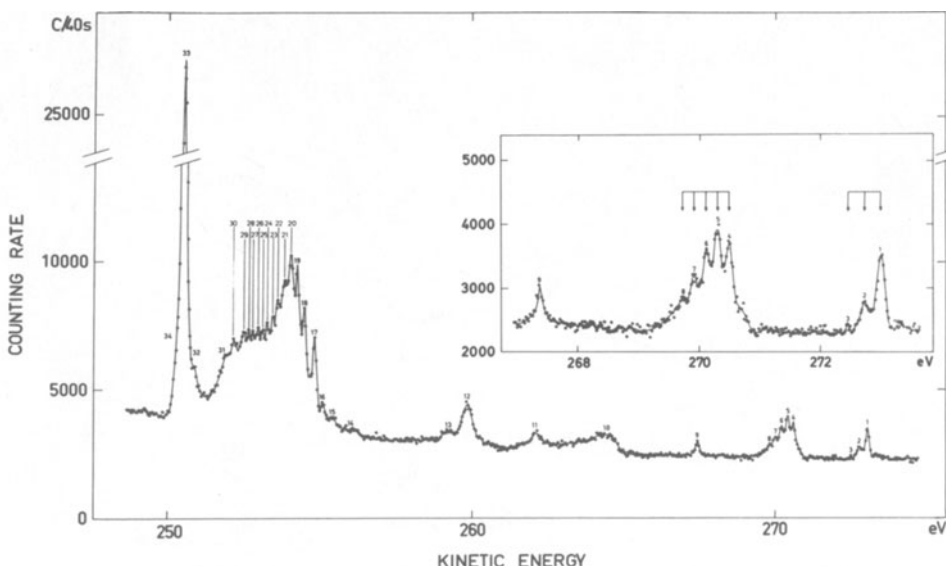


FIGURE 6.12. Details of vibrational structure in the carbon K - LL Auger spectrum of CO. [Reproduced from Siegbahn *et al.*,⁽⁴²⁾ Figure 5.28.]

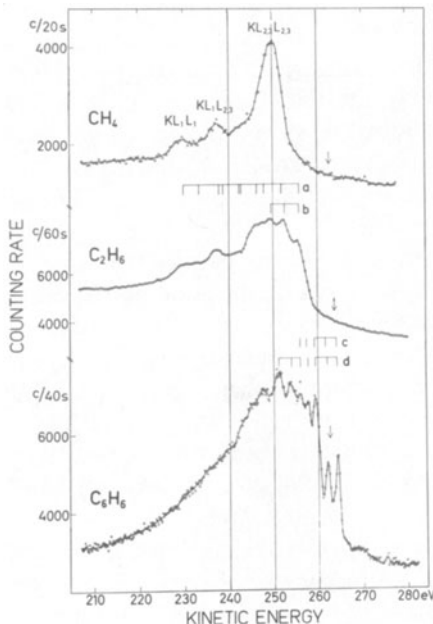


FIGURE 6.13. Comparison of K - LL Auger spectra for methane, ethane, and benzene. As one goes from methane to benzene the dissociation energies become less and the sharpness of the Auger line increases. [Reproduced from Spohr et al.,⁽⁵³⁾ Figure 5.]

dissociative energy for methane, ethane, and benzene is estimated to be, respectively, -13, -8, and +1 eV, and the line broadening may also be expected to decrease in that order. The relative sharpness of the lines observed in the bromomethane compounds was also interpreted in terms of whether the Auger transitions involve bonding orbitals leading to dissociative states.

Recently, detailed analyses have been carried out on the high-resolution Auger spectra of H_2O ,⁽³⁷⁾ HF ,⁽⁵⁴⁾ and C_2O_3 .⁽⁵⁵⁾

3.3. Study of Ionization Phenomena by Auger Spectroscopy

In the previous sections on Auger spectroscopy of gases we have emphasized the nature and identification of the various Auger lines. Our aim was to obtain the correct analysis of the observed Auger process. In obtaining this analysis we learned that many of the lines were satellite lines, which arose from some form of initial excitation. These lines can thus be used as a means for following the nature of the excitation process.

We have already discussed in some detail the information gained on the nature of K -hole excitation states as the result of electron impact. Glupe and Mehlhorn⁽⁵⁶⁾ used the Auger spectra of C, N, O, and Ne to determine the K -shell ionization cross section as a function of electron impact energy. The

nature of electron shakeoff has been studied by Auger spectroscopy. Krause *et al.*⁽⁵⁷⁾ showed that the satellite spectra for neon representing initial shakeoff and shakeup processes were essentially identical whether produced by electron impact or photoionization. By examining the satellite lines relative to the normal Auger lines, Carlson *et al.*⁽⁵⁸⁾ studied the extent of electron shakeoff as a function of electron impact energy. From these studies it became clear that electron shakeoff as the result of inner shell ionization by electron impact could be treated by the sudden approximation, just as with photoionization.

Rudd,⁽⁵⁹⁾ using Auger spectroscopy, followed the nature of ionization by protons and found, in marked contrast to photoionization and electron impact, much larger contributions from satellite lines than would be predicted by the sudden approximation. Recent studies, however, by Stolterfoht and co-workers⁽⁶⁰⁾ show that as the proton energy approaches 500 keV the Auger spectrum approaches that produced by electron impact. That is, at these higher energies the region of the sudden approximation is reached, and the probability for initial multiple ionization is governed by the laws for electron shakeoff in which only the creation of an inner shell vacancy matters, not how that vacancy was formed. From Figure 6.14 we see that the relative intensities of the regions A, B, C, and D for nitrogen remain the same with projectile energy. These are the normal Auger processes, which do not depend on multiple ionization. Region B' increases in relative importance as the energy of the proton decreases. This region must be due to multiple ionization; and, in fact, Moddeman *et al.*⁽⁴⁸⁾ had previously suggested that the region B' might be due to KW-WWW transitions. The increase of multiple ionization with lower proton velocity suggests a direct collision mechanism. The use of proton bombard-

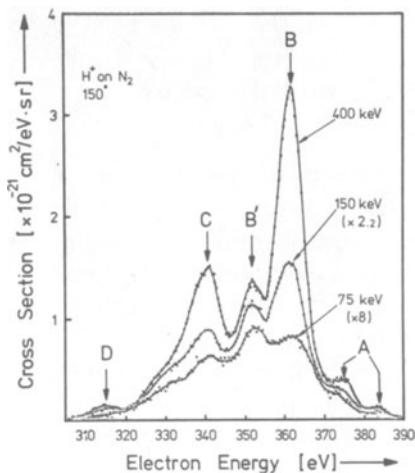


FIGURE 6.14. Comparison of N_2 K-LL Auger spectra as a function of kinetic energy of impact protons. B' arises from multiple ionization and its intensity relative to the other portions of the Auger spectrum changes with impact energy. [Reproduced from Stolterfoht *et al.*,⁽⁶⁰⁾ Figure 1.]

ment with varying energy could be of substantial value in helping to distinguish which areas of the Auger spectrum arise from normal Auger processes and which are due to initial multiple ionization.

If an ion is used as a projectile, the ionization it produces will be influenced by the atomic behavior of electrons surrounding the ion unless the ion moves at velocities that are far in excess of electron orbital velocities, which for protons would be far in excess of 20 keV. The present interest in the nature of multiple ionization by high-energy heavy ions could be assisted by Auger spectroscopy. Auger energies in highly charged ions will shift from that observed for an ion with a single inner shell vacancy. From both the Auger energies and relative intensities of Auger peaks one can in principle analyze the extent of ionization and excitation for a given heavy ion. Both the target and projectile could be so analyzed. This type of analysis has been applied extensively to the x rays of highly charged ions,* and could be profitably made using Auger spectra. In fact, Auger energies are more sensitive to the removal of outer shell electrons than is the case with x-ray energies. One drawback is that electrons are more susceptible to recoil energy than photons, and considerable broadening due to Doppler shifts may arise from electron emission from a recoiling heavy ion. Nevertheless, increasing use has been made of Auger spectroscopy in the study of ion-ion collisions.⁽⁶²⁾

3.4. Autoionization

When an atom is placed in an excited state which is above the ionization potential, the atom may readjust by a nonradiative process with the ejection of a discrete-energy electron. When excitation occurs only with valence electrons, this process is generally known as autoionization rather than as an Auger process, the latter name being restricted to situations containing a vacancy in the core shells. However, the nature of the Coulombic readjustment is physically identical for the two phenomena.

It is not the purpose of the book to cover the vast amount of material on autoionization, but rather to point out its similarity with Auger spectroscopy. In particular, the studies carried out by Siegbahn *et al.*⁽⁴²⁾ on the rare gases using 4.0-keV impact electrons to create the excitations and an electron spectrometer to record the discrete-energy electrons are identical in experimental procedures to Auger spectroscopy, except that the energies are lower. Figure 6.15 shows a typical example of the autoionization spectra for Ar. Helium, Ne, and Xe were also studied by these authors. The dips in the spectra are caused by the interference between a discrete autoionization state and the continuum.

* See Ref. 61 for a general review of multiple ionization arising from ion collisions and the use of x-ray spectra for studying the process.

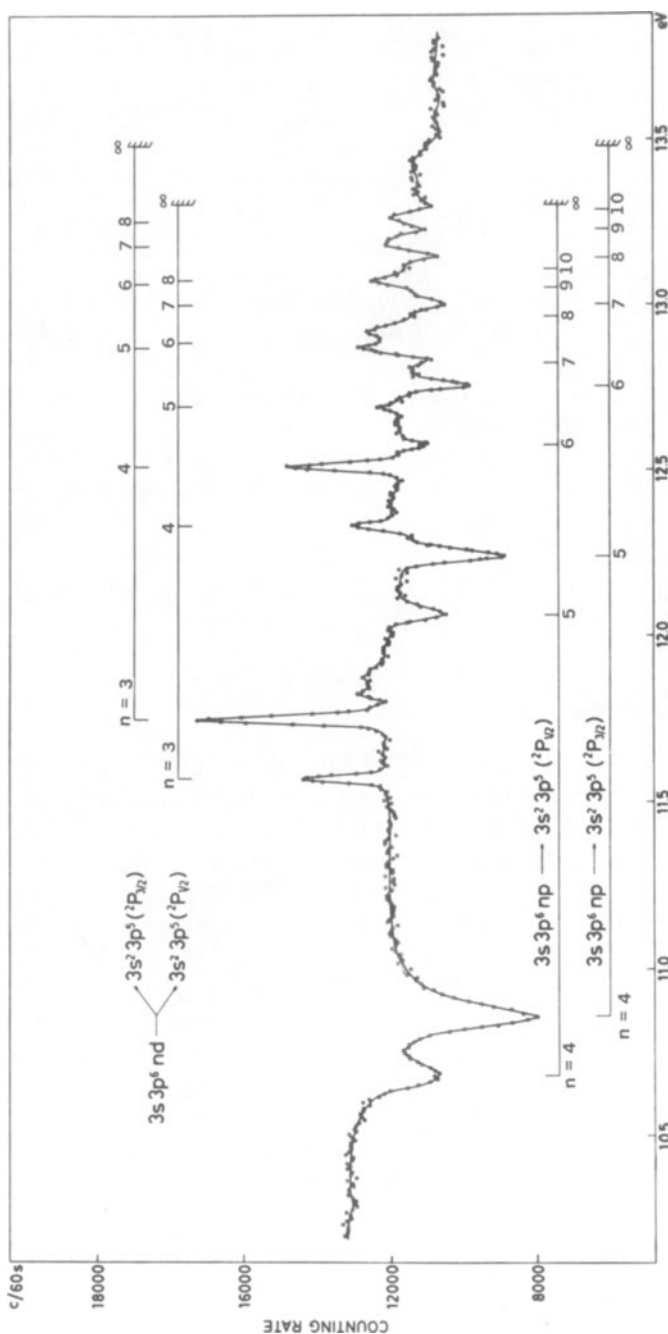


FIGURE 6.15. Autoionization electron spectrum from argon. Initial excitation created by high-energy electron impact. [Reproduced from Siegbahn *et al.*, (42) Figure 4.6.]

Good agreement was obtained with photoabsorption measurements, although some observed lines formed by electron impact are forbidden for photoabsorption.

Another area of recent interest has been the study of discrete-energy electrons ejected from an ion which has passed through a thin foil. If the ion as the result of passing through the foil is excited into a metastable state, the state may decay during its flight by autoionization. Lucas and Harrison⁽⁶³⁾ have discussed such measurements for an incident 291-keV N⁺ beam. Sellin *et al.*⁽⁶⁴⁾ have studied a number of highly charged ions for autoionization, using ions with high kinetic energy as projectiles. For example, Cl¹⁴⁺ and Ar¹⁵⁺, which are lithiumlike in configuration, have been studied. By examining the autoionization processes during flight, they have also been able to ascertain the half-lives of the excited states.

3.5. Auger Spectroscopy for Use in Gas Analysis

Auger spectroscopy offers a number of advantages for gas analysis. Figure 6.16 shows oxygen *K*-*LL* Auger spectra from four different molecules. Though the center of the spectrum in each case is approximately 490 eV, indicating that we are dealing with the element oxygen, the details of the spectra are quite dissimilar, yielding essentially "a fingerprint" for a given molecule. Thus, an Auger spectrum offers both an elemental analysis and molecular identification.

Auger spectra of gases often reveal lines with very small natural widths. There is no line broadening from the excitation source, as with photoionization. The principal limitation to resolution comes from the natural widths of the core levels. In the case of carbon this has been shown to be less than 0.2 eV. From calculations on the lifetime for *K* vacancies the natural width for all elements in the first row ought to be less than 0.2 eV. The state of the doubly charged molecular ions following an Auger process should also be stable for at least 10⁻¹⁴ sec if the line broadening is not to be increased, but many molecules should be able to meet this requirement. The intensity of producing Auger lines by electron impact can be made very high. It is easy to produce electron beams of 500 mA. I have found that a beam of only 0.5 mA would produce Auger lines with intensities whose limitation was the saturation of the electron multiplier (~50,000 counts/sec) when the pressure of the target gas was about 10 μ m. For higher rates a current integrating device can be used. The peak-to-background ratio is an important consideration if high sensitivity is being sought (parts per million). When x rays were used to produce inner shell vacancies, ratios as high as 30,000 to 1 were obtained. When electron impact was used, the best ratio was 500 to 1, and the importance of scattered electrons increased as one went to lower kinetic energies. However, with greater care for

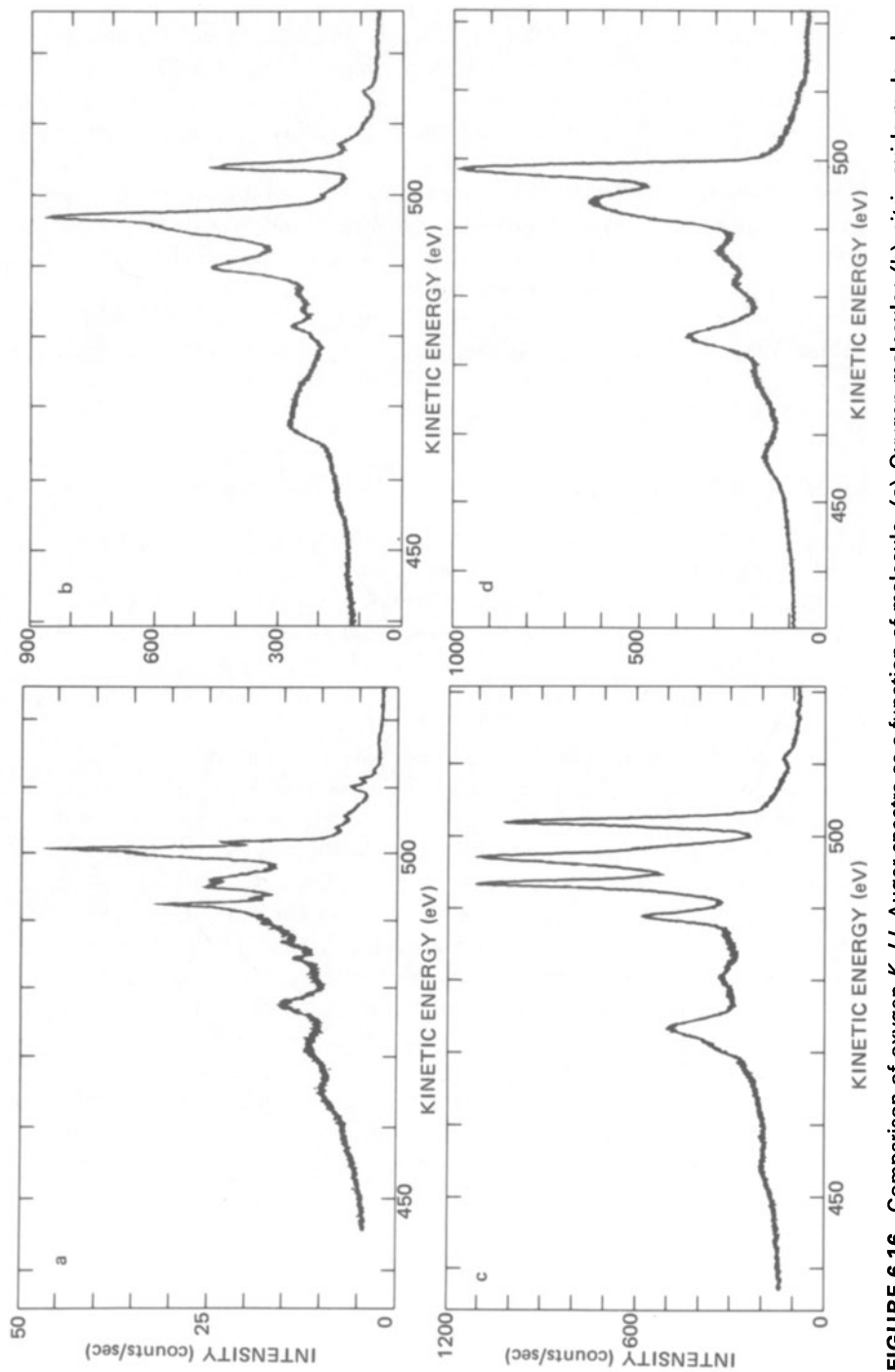


FIGURE 6.16. Comparison of oxygen K_{LL} Auger spectra as a function of molecule. (a) Oxygen molecule; (b) nitric oxide molecule; (c) carbon dioxide molecule; (d) water molecule. [Data taken from Modderman *et al.*⁽⁴⁸⁾]

reducing secondary electrons, the peak-to-background ratios might be substantially improved.

There are limitations in the use of Auger spectroscopy as an analytical tool for gases. To analyze two or more molecules (say hydrocarbons) simultaneously by studying the Auger spectra of a common element (carbon) would be difficult, since the spectra would overlap. If the gases were present to about the same order of magnitude, and their spectral profiles well known, analysis would be possible, but not for trace amounts. A trace element might be studied, however, without interference, conceivably to a few parts per million. The use of Auger spectroscopy can be greatly enhanced by combining it with gas chromatography, as has been accomplished with mass spectroscopy.

Good resolution, high counting rates, unique identification of molecules, and sensitive elemental identification all make Auger spectroscopy a potentially powerful tool for gas analysis. As yet, no systematic study of its analytical possibilities on gases has been made, but it would appear to be a worthwhile undertaking.

4. USE OF AUGER SPECTROSCOPY IN THE STUDY OF SOLIDS

The practical application of Auger spectroscopy as a tool for elemental analysis on surfaces has been so successful as to almost isolate these endeavors from other applications of Auger spectroscopy. Before undertaking a discussion of surfaces, there are several smaller topics on solids which require our attention. First, there are some problems with AES which are peculiar to solids. These concern, for example, (1) the practical differences between measuring Auger lines in solids when initiating inner shell vacancies by x rays and impact electrons, (2) the presence of high energy Auger lines in solids, (3) characteristic energy losses in solids, and (4) charging of nonconducting materials.

Second, we shall examine those studies that have stressed the nature of the Auger spectrum itself rather than the information it can yield about the surface. These studies have eschewed cleanliness for high resolution. Most surface studies have put the emphasis on cleanliness of the surface, accepting rather modest resolution. Recent improvements in technology have made the decision of cleanliness versus resolution unnecessary, but it is still present in much work. In any case there exists an interest in AES of solids that lies outside of surface science and needs separate treatment. Finally, the use of Auger spectroscopy as an analytical tool for solids, again outside the special domain of surface interest, will be discussed.

When we do turn our attention to surfaces, we shall discuss the types of

information about the surface that can be obtained with Auger spectroscopy, giving numerous examples from the recent literature. Comparison will then be made between AES and PES as a surface tool. Also, other competitive methods of surface analysis will be briefly discussed and compared with AES.

4.1. Special Problems Encountered on Using AES with Solids

4.1.1. Variables Concerned with Production of Auger Electrons

One may create an inner shell vacancy through a variety of methods, including irradiation with electrons and x rays. Haas *et al.*⁽⁶⁵⁾ have used argon ions to excite the Auger spectrum of Al metal. Electron impact is usually used for producing Auger lines for analytical purposes. It provides an intense beam which can also be brought to a fine focus. X irradiation has its value in providing less radiation damage and (under some conditions) better peak-to-background ratios. Barrie and Brundle⁽⁶⁶⁾ have explored the practical problems of measuring Auger spectra from CO adsorbed on Mo induced by both electron impact and soft x rays. Pessa⁽⁶⁷⁾ has studied the problem of peak to background using electron impact versus Al $K\alpha$ radiation. Figure 6.17 shows some of his results using 5-keV electron impact. The abscissa is the Auger energy and the ordinate is

$$S = \frac{(I_m - I_b)_x / (I_b)_x}{(I_m - I_b)_e / (I_b)_e} \quad (6.9)$$

where I_m and I_b are the peak and background intensities for x rays (x) and electron impact (e). For Auger processes with energies below 500 eV, electron impact seems superior, but above that figure, Al $K\alpha$ x rays give a better performance. Figure 6.18 shows a signal-to-noise ratio $[(I_m - I_b)/I_b]_e$ as a function of electron impact energy.

Neave *et al.*⁽⁶⁸⁾ and Gallon⁽⁶⁹⁾ have studied the role played by back-scattered electrons in the production of Auger peaks. They concluded that a sizable fraction of the Auger electrons usually observed came not from ionization created by the primary beam of impact electrons, but from back-scattered electrons. Neave *et al.* also pointed out the particular importance that backscattered electrons play in the production of Auger electrons as a function of glancing incidence of the initial beam. Figure 6.19 contrasts Auger yields as a function of initial impact energy and angle of incidence.

Staib⁽⁷⁰⁾ has compared relative intensities of $K-LL$ Auger lines for O, Al, and Si and the $L-MM$ lines from potassium under the controlled conditions of looking at only the top layers of a cleaved mica sample where the positions

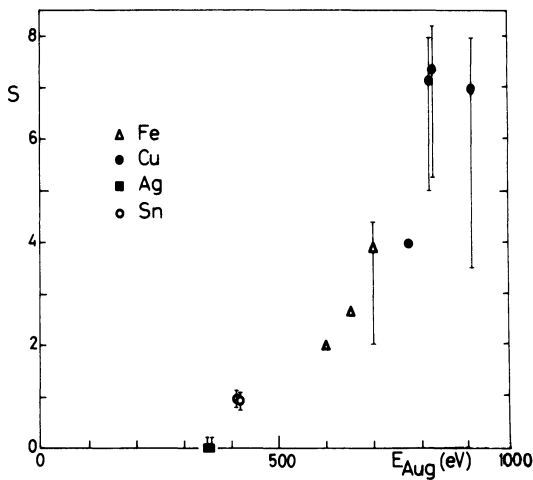


FIGURE 6.17. Peak height ratio S [cf. equation (6.9)] vs Auger energy for Fe, Cu, Ag, and Sn. Sn. Electron impact energy is 5 keV. [Reproduced from Pessa,⁽⁶⁷⁾ Figure 3.]

of the different atoms are known from crystallography. Results are compared with the semiempirical formula of Darwin.

The angular dependence of Auger emission from a copper 111 surface has been studied by Holland *et al.*⁽⁷¹⁾ They found marked crystallographic

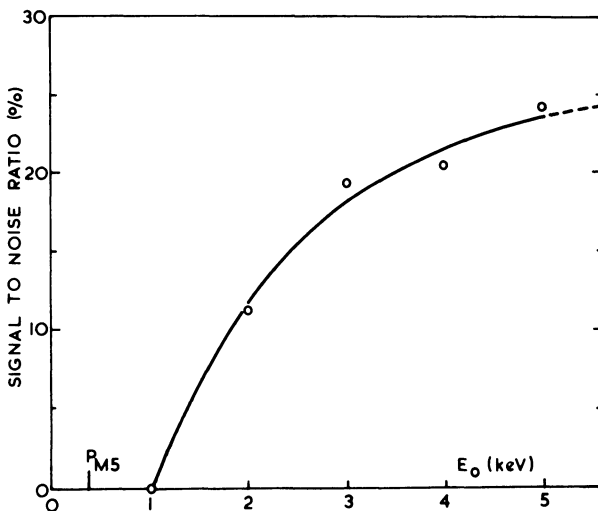


FIGURE 6.18. Signal-to-noise ratio of the 350.5-eV $M_5N_{4.5}N_{4.5}$ Auger line from Ag metal vs kinetic energy of primary electrons. [Reproduced from Pessa,⁽⁶⁷⁾ Figure 1.]

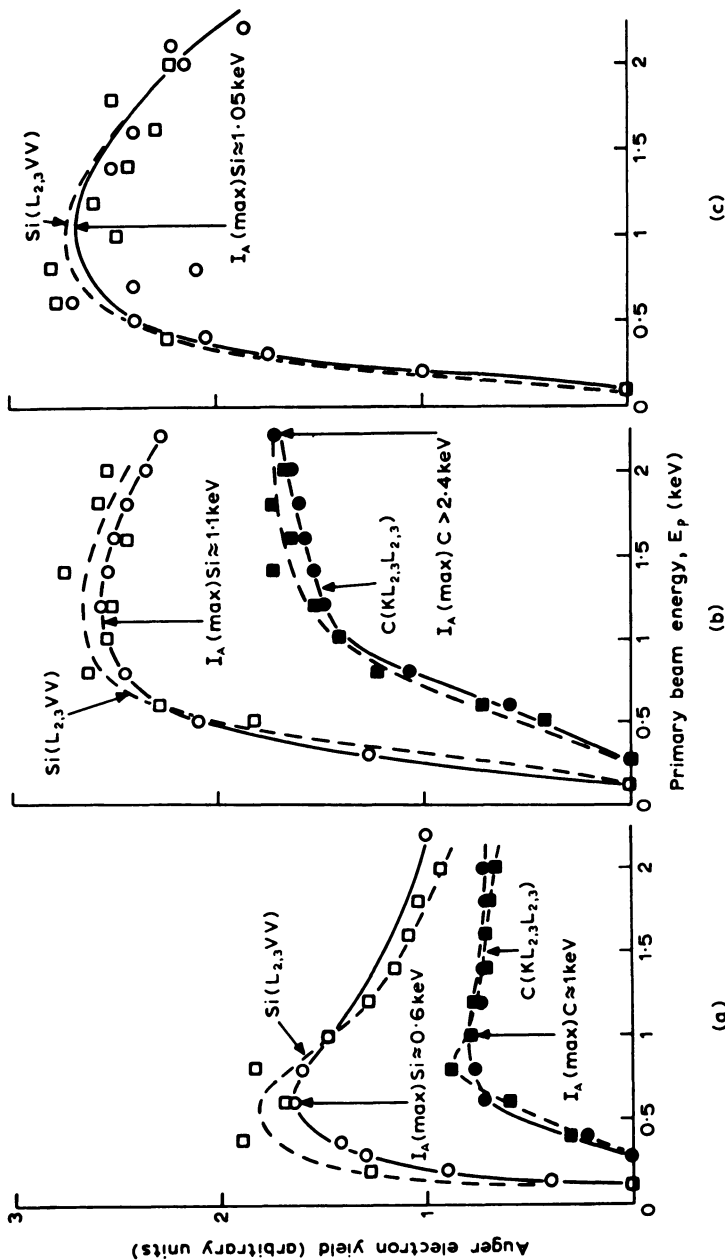


FIGURE 6.19. Measured intensity of Auger electrons as a function of primary beam energy at normal and glancing incidence and with constant beam current or constant target current. (a) Normal incidence, constant beam current ($1 \mu\text{A}$) ; (b) glancing incidence (20°), constant beam current ($1 \mu\text{A}$) ; (c) glancing incidence (20°), constant target current ($0.8 \mu\text{A}$). For Si : (○) observed; (□) predicted. For C : (●) observed; (■) predicted. Constant rms voltage 2.5 V. [Reproduced from Neave *et al.*, (68) Figure 1.]

dependence, and feel that such analyses could provide new information on the valence electron wave functions in the surface region of the solid.

4.1.2. High-Energy Satellite Lines

High-energy satellite structures have been observed in the Auger spectra of solids.⁽⁷²⁾ This has been interpreted by Chung and Jenkins⁽⁷³⁾ and others⁽⁷⁴⁾ as being due to plasmon gains. Pattinson and Harris feel the plasmon gain mechanism is unlikely.⁽⁷⁵⁾ It is more likely that the high-energy lines arise from an initial multiple ionization⁽⁷²⁾ or perhaps resonance absorption as observed in the gas phase. (Cf. Section 3.2.) The question of Auger satellites in solids is still under active consideration.⁽⁷⁶⁾

4.1.3. Characteristic Energy Losses

Electrons ejected from a solid can suffer characteristic energy losses, usually due to plasmon losses. Since Auger spectra are generally rather complex and often not well resolved and are spread over a considerable range of energies, peaks from characteristic energy losses are much more difficult to disentangle from the normal Auger spectrum than is usual in the case of photo-electron spectroscopy. Also, surface contamination will alter the nature of the characteristic loss peaks considerably.

4.1.4. Charging in Nonconducting Samples

Charging as the result of an impinging beam of electrons on a nonconductor is a particularly severe problem in Auger spectroscopy. Often the charging and instability of the charged surface will prevent a meaningful Auger spectrum. However, this problem can be overcome by choosing the proper angle of incidence and bombarding energy. The important factor is the ratio δ (the number of secondary electrons leaving the target to the number impinging on the target). If $\delta = 1$, the charge is stabilized; if <1 , the charge is negative, and if >1 , positive. Goldstein and Carlson⁽⁷⁷⁾ have worked on this problem with glass surfaces. They found the best spectra are taken when δ is initially >1 and stabilizes to a slightly positive charge, which prevents some of the secondary electrons from leaving. To obtain $\delta > 1$, a grazing incidence angle of 10° was used. (The smaller the grazing angle, the greater chance there is for secondary electrons to leave.) The choice of impact energy is also important, δ becoming less than 1 if the energy of the impinging beam of electrons is either too large or too small. In this case the primary beam needed to be between 1.5 and 3.0 keV.

4.2. High-Resolution Auger Spectroscopy with Solids

In this section we shall discuss use of Auger spectroscopy with solids in areas of interest other than surfaces. In addition, attention will be concentrated on data taken with high-resolution analyzers, and on those spectra whose energies are sufficiently low that instrumental broadening and broadening from the natural widths of shells do not exceed a net resolution of a couple of volts. Auger spectra accompanying nuclear decay have received a fair degree of attention in the past from beta spectroscopists (e.g., Ref. 5) and although the data were of great help in providing a basis for understanding the Auger process, they are generally not of practical interest to the chemist.

Fahlman *et al.*⁽⁷⁸⁾ studied a number of light elements using either metals (Na, Mg) or simple salts (KCl, K₂SO₄, Na₂S₂O₃) and Albridge *et al.*⁽⁷⁹⁾ added to these studies work on alkali metals and alkaline earth fluorides. Also, high-resolution studies have been done on the *M-NN* Auger spectra of Ag, Cd, In, Sb, and Te metals and NaI.⁽⁸⁰⁾ These spectra, not surprisingly, showed more the character of free elemental ions than molecular orbital structure (cf. Figure 6.20). Some variation in the fluoride spectra due to chemical environment was found. For example, the *K-L_{II, III}L_{II, III}* ¹D transition was 654.6, 654.4, and

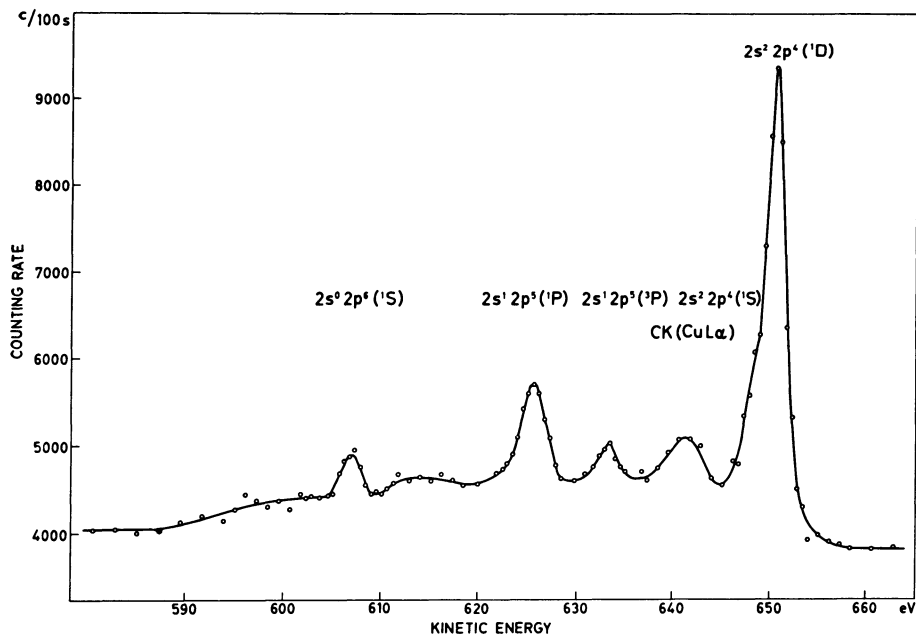


FIGURE 6.20. The *K-LL* Auger spectrum of fluorine in sodium fluoride using Cu(*L*) x rays as excitation source. [Reproduced from Albridge *et al.*,⁽⁷⁹⁾ Figure 2.]

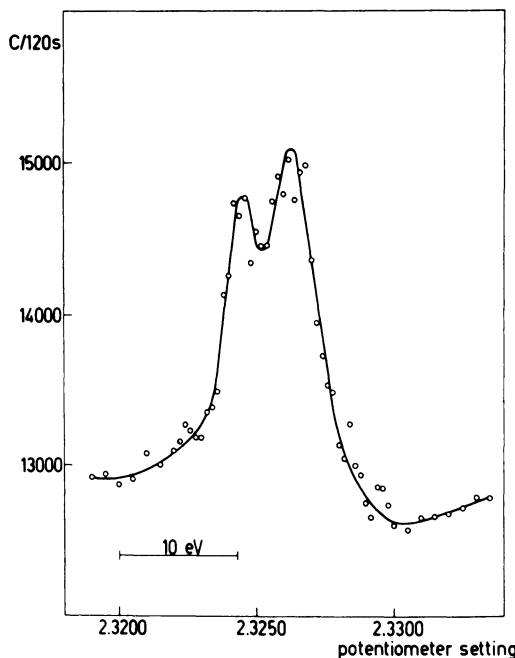


FIGURE 6.21. Spectrum of the $KL_1L_1(^1P_1)$ normal Auger line from KCl and its low energy satellite. [Reproduced from A. Fahlman, K. Hamrin, G. Axelson, C. Nordling, and K. Siegbahn, *Z. Phys.* **192**, 484 (1966), Figure 2.]

657.3 for salts whose cations were Na, Li, Mg. In addition, there was variation in the broadening of the fluoride spectra. Besides the normal Auger spectra, satellite lines were found at energies slightly lower than the normal lines (Figure 6.21). These lines probably arise from some phenomenon similar to that discussed in Section 2.2, such as electron shakeoff. What is surprising here are the relatively large intensities. The $K-LL$ spectrum of oxygen from TiO_2 indicates a more complex Auger spectrum than that deduced from only atomic considerations.

The experimental Auger spectra for solids are less satisfactory than the corresponding spectra of gases with regard to resolution and peak-to-background ratio. Line broadening in solids may be due to the more complex band structure or to experimental problems associated with the charging up of nonconductors. The poor peak-to-background ratios with solids are due to the unavoidable secondary electrons from inelastic scattering. The spectra are generally better when the initial inner shell vacancies are created by γ radiation than by electron impact. Interference from plasmon loss peaks as produced by

the higher energy Auger electrons presents a problem for measuring the lower energy Auger spectra. Still a great deal of added information other than element identification is possible with high-resolution Auger studies on solids.

Kumar⁽⁸¹⁾ has carried out a detailed study on the $L-MM$ Auger spectra from solid compounds of germanium. High-resolution KLL spectra for Mg⁽³⁷⁾ and Al⁽³⁸⁾ and their respective oxides have been taken using Al $K\alpha$ and Ag $L\alpha$ x rays for creating the initial core holes. Powell and Mandl⁽⁸²⁾ have observed the $L_{III}-M_{II}, III M_{IV}, v$ spectrum of nickel and copper with high resolution. The data reveal new structure, which was correlated in part with the final states for atomic Cu and in part with features of the $3d$ band density of states as determined by soft x-ray emission spectroscopy and x-ray photoelectron spectroscopy. Yin *et al.*⁽⁸³⁾ also measured some fine structure in the $L-MM$ Auger spectra of Cu and Zn. Wagner,⁽⁸⁴⁾ using Al $K\alpha$ x rays for producing Auger lines, studied a wide variety of compounds, including 44 different elements. Instrumental linewidths were from 0.5 to 1.0 eV. Strong chemical effects were noted for the shapes, intensities, and energies of some of the Auger lines. Schön⁽⁸⁵⁾ has observed triplet-singlet splitting in the copper Auger spectrum and Bassett *et al.*⁽⁸⁶⁾ have found fine structure in silver and indium indicative of spin-orbit splitting in the initial state and multiplet structure in the final state. Jørgensen and Berthou⁽⁸⁷⁾ have related multiplet splitting in the Auger spectrum of copper(I) and silver(I) to the effects of linear ligand fields.

4.3. General Analytical Use of Auger Spectroscopy

Although both PESIS and AES are surface measurements, photoelectron spectroscopy has been used extensively to study bulk properties, with lesser emphasis on surface properties, while the reverse is true for Auger spectroscopy. The more complex Auger spectra are harder to measure and interpret for chemical shifts, and studies using electron bombardment on nonconducting solids are difficult because of the extensive charging. A comprehensive analytical tool must obviously be able to handle more than just conductors. The above problems can be overcome in Auger spectroscopy and the advantage of high signal response leading to a rapid analysis makes AES a valuable tool for general analytical purposes.

As will be obvious from Section 4.4.2.5, the interest in chemical shifts in Auger spectroscopy of solids is rapidly growing. This growth will certainly be enhanced by the availability of Auger spectrometers with high resolution. The problem of charging for nonconducting samples may be overcome by the proper choice of grazing incidence radiation and energy of the electron impact beam (cf. Section 4.1.4.).

As an example of the use of AES in general analysis, see the work of Connell *et al.*⁽⁸⁸⁾ on some lunar samples. Carter *et al.*⁽⁸⁹⁾ have appraised the

relative merits of PESIS and AES in analyzing particulate matter. Whereas photoelectron spectroscopy requires from 30 min to a day for a complete detailed analysis, Auger spectra can be taken in seconds. However, because of the greater complexity of Auger spectra and overlapping of Auger lines from different elements, it was not possible to unambiguously detect some of the elements. For example, it is generally not possible to determine lead from its low-energy Auger spectrum, because of interferences, and one has to use impact electrons with energies of 5 keV or greater in order to excite the higher energy Auger lines. Also, since the peak-to-background ratio is generally poorer in Auger spectroscopy, the sensitivity for elements in low concentration is not as good. Charging is a major problem and the requirement for a low grazing incidence means the analysis must confine itself close to the surface. Auger spectroscopy is also not as successful in measuring the chemical state of, for example, the nitrogen and sulfur compounds as is PESIS. However, in spite of limitations, Auger spectroscopy should still be quite valuable as a general analytical tool for studies other than surface work.

4.4. Use of Auger Spectroscopy in the Study of Surfaces

4.4.1. General Considerations

The first use of Auger spectra to aid in the analysis of surfaces was made by Lander⁽⁹⁰⁾ in 1953, who studied various surfaces with low-energy electrons (500–1000 eV) and measured the resultant Auger electrons that were emitted. The recent interest, however, was kindled by Scheibner and Tharp⁽⁹¹⁾ and Weber and Peria,⁽⁹²⁾ who coupled Auger spectra measurements to a conventional low-energy electron diffraction (LEED) system. Since that time hundreds of papers have appeared using Auger spectroscopy as a tool for surface analysis.*

Since the use of Auger spectroscopy for studying surfaces has come primarily from the work of surface scientists, more attention has been placed on surface cleanliness than high resolution. In contrast, photoelectron spectroscopy has been more concerned with better resolution. One field may be said to be clean but imprecise, the other accurate but dirty. Actually, technology is capable of achieving both goals. Physical Electronics now markets an Auger instrument capable of 0.05% instrumental resolution of the initial kinetic energy, which still holds the vacuum in the 10^{-10} Torr region. We can expect to see more and more use of high-resolution AES in surface analysis.

The choice of an analyzer to be used in Auger studies with LEED was dictated by the needs for simplicity and high transmission and the limitations

* See Ref. 93 for a bibliography and Ref. 94 for reviews of this area.

placed by the desire for surface cleanliness. Thus, a retarding grid device was chosen (cf. Chapter 2, Section 2.2.1 for further description). The energy resolution of such a device is usually from 3% to almost 0.3%. One of the biggest handicaps of taking data by the retarding grid method is that the signal is accumulative. Even modulation of the signal still makes analysis of details of some of the lower-energy lines difficult. Since Auger data taken with a retarding grid spectrometer are plotted in terms of the differential intensity, a single Auger line has both a maximum and a minimum. By convention the energies for various lines are usually taken at the minimum.

The detector for the LEED type of retarding grid analyzer must be, by virtue of its geometry, an electrostatic collector. One obvious advantage for a dispersion instrument is that it can focus its signal on an electron multiplier. Thus, each electron event can be individually detected and recorded. In addition, the development of dispersion instruments with high transmission has removed the advantage of the large-solid-angle analysis capability of the retarding grid method.

However, whereas the LEED Auger spectrometers may be open to criticism with regard to the most effective energy analysis, workers in this field have been most studious in their development of clean vacuum systems and in surface preparation. See Chapter 2, Section 1.2.2 for details on obtaining clean surfaces. A pressure of at least 1×10^{-9} Torr is needed if one wishes to prevent complete coverage of the surface in 1 h. Much of the LEED-Auger work is done in the 10^{-10} Torr range or lower.

Modern Auger spectrometers with dispersion analysis have more than ample intensity. Thus, they still collect their signal on an electrostatic accumulator. The signal is processed electronically and is presented in a differentiated form. Grant *et al.*⁽⁹⁵⁾ have suggested processing the data electronically by first differentiating and then integrating back the spectrum. The background, which can usually be represented by a polynomial, is removed by such a procedure, while the signal is restored to its original form. The Auger spectra thus processed have a better peak signal-to-noise ratio, and the intensities of the peaks are easier to compare quantitatively in the integrated form.

As an analytical tool, Auger spectroscopy is quite successful for the lighter elements, particularly the first row elements from $Z = 3$ to 10. The fluorescence yield is less than 1%, so that these elements are difficult if not impossible to measure by use of their characteristic x rays. The K vacancies are filled in nearly every case by an Auger process. In addition, the K-LL Auger spectra are relatively simple and quite distinctive as to the element involved. However, any element can be studied (except H and He) by Auger spectroscopy and researchers have now extended the method throughout the periodic table. Comprehensive tables based on atomic binding energies have been prepared⁽⁹⁾ for all Auger transitions for energies between 10 and 3000 eV for elements up

to $Z = 103$. Comprehensive experimental data for most of the elements have also been reported.⁽¹⁵⁾

Auger spectroscopy for surface analysis has been used primarily for qualitative analysis. It is quite sensitive; 1–2% of a monolayer can generally be detected, and in some cases as little as 0.2–0.5% has been reported. The sensitivity in fact is limited by surface cleanliness rather than signal strength, since the cleanliness depends on time of exposure. It is also important to note that Auger spectra can be taken in milliseconds. In general, the cross section for inner shell ionization, and thus the sensitivity for detection, decreases with increasing binding energy. Therefore, the lower energy Auger processes that are still characteristic for a given element are the ones usually chosen for study, because of the greater cross section for producing these Auger processes and because such low-energy Auger electrons will emanate from layers closer to the surface.

Quantitative analysis is in principle also possible. The quantitative aspects of Auger spectroscopy have been discussed by Seah.⁽⁹⁶⁾ Meyer and Vrakking⁽⁹⁷⁾ have studied C, N, O, P, S, and Cl for quantitative analysis, combining AES with ellipsometry. Staib and Kirschner⁽⁹⁸⁾ have determined absolute atomic densities using Auger electron spectroscopy. The relative intensities depend on a number of variables: inner shell ionization cross sections, Auger transitions rates, and inelastic scattering of the emitted Auger electrons. The problems, in fact, are similar to those encountered in the use of PESIS for quantitative analysis. However, with careful calibration, one ought to be able to obtain quantitative analysis of a sample, assuming homogeneity, to an accuracy of about 10%. If the sample is not homogeneous at the surface, auxiliary experiments will have to be made before a final interpretation is reached. Use of Auger spectroscopy in quantitative analysis is not a precise measurement, but it can still be of great help in studying the surface.

To emphasize the surface layers, the angle between the electron beam and the surface plane of the target is made as small as possible (usually about 10°). By changing the grazing angle of the electron beam, one can vary the relative contributions of the surface layers, and thus determine if there is any inhomogeneity of the chemical composition of the surface layers. This information could also be correlated with studies of the relative intensities for Auger electrons and photoelectrons having different energies and different mean free paths, as discussed in Chapter 5, Section 5.2. Meyer and Vrakking⁽⁹⁹⁾ have shown that it is also possible to gain some in-depth information by variation of the energy of the primary impact electron.

One of the chief advantages of Auger spectroscopy as an analytical tool for solids is that a small but intense beam of electrons can be used to survey the sample. A normal electron beam has a current from 10 to 100 μA with a focal spot of less than 1 mm diameter. Thus, individual small portions of the surface

can be studied one at a time. Spatial resolution for Auger analysis has been achieved for areas smaller than 1 μm in diameter⁽¹⁰⁰⁾ (cf. Figure 6.22). Auger spectroscopy has been wedded with other methods of surface analysis, such as LEED (Low Energy Electron Diffraction) and electron microscopy, so as to yield elemental analysis and structural information simultaneously.

4.4.2. Literature Survey of Surface Applications

A complete literature survey of the use of Auger spectroscopy for surface analysis will not be attempted here (see Refs. 93 and 94), but a sufficient number of examples will be cited to illustrate the scope of the field.

4.4.2.1. Surface Impurities. Auger spectroscopy can detect foreign elements down to about 1 % of a monomolecular layer. For bulk analysis Thomas and Morabito⁽¹⁰¹⁾ found that the detectable limits for boron and phosphorus translate into about 8×10^{18} atoms/cm³ when mixed with silicon. Auger spectroscopy has become one of the criteria for surface cleanliness. For example, in the study of methods for surface cleaning, it has been found that although electrical heating removes oxygen and carbon from nickel⁽¹⁰²⁾ and steel,^(102, 103) it also promotes diffusion of sulfur to the surface. Jenkins and Chung⁽¹⁰⁴⁾ found both carbon and sulfur diffused to the surface on heating of copper. Taylor⁽¹⁰³⁾ and Sickafus⁽¹⁰⁵⁾ demonstrated ion bombardment as a preferable method for cleaning the transition metals. Lambert *et al.*⁽¹⁰⁶⁾ studied the carbon overlay on Pt and also warned about the problem of cleaning Pt by heating.

Lassiter⁽¹⁰⁷⁾ studied contaminants as polycrystalline silver and Dufour *et al.*⁽¹⁰⁸⁾ examined the surface of high-purity magnesium and aluminum crystalline specimens.

4.4.2.2. Surface Coverage. Detailed studies can be made by Auger spectroscopy on the way in which surfaces are covered. For example, Weber and Johnson⁽¹⁰⁹⁾ measured the degree of deposition of K ions into silicon and germanium from 0.1 to 1.0 of the first surface layer, finding a linear relationship. Palmberg⁽¹¹⁰⁾ discovered that the sticking coefficient of Xe on palladium (100) was independent of surface coverage up to 5.8×10^{14} atoms/cm² and then decreased suddenly to zero. A study of the adsorption of oxygen on tungsten was made by Musket and Ferrante.⁽¹¹¹⁾ Pollard⁽¹¹²⁾ investigated the growth of thorium on the tungsten (100) plane. The tungsten Auger peak was found not to be covered by thorium even after an equivalent of 25 monolayers was deposited. The conclusion was that the thorium nucleated so as to cover only 5 % of the total surface.

Joyce and Neave⁽¹¹³⁾ studied the interaction of oxygen on silicon, obtaining a sticking constant of 8×10^{-4} , which was independent over 10^{-5} – 10^{-8} Torr. The adsorption was found to be initially rapid, followed by a substantial change in rate as the monolayer neared completion.

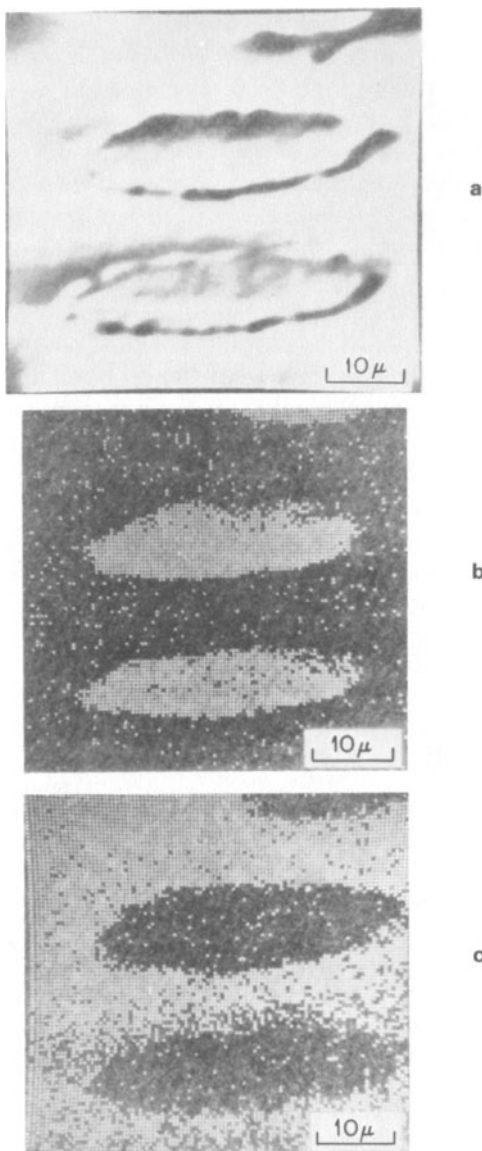


FIGURE 6.22. Study of iron-copper composite sample using scanning electron microscope: (a) secondary electron micrograph, (b) Auger image of iron (oval), (c) Auger image of copper (background). [Reproduced from MacDonald and Waldrop.⁽¹⁰⁰⁾]

Bonzel⁽¹¹⁴⁾ carried out careful studies on the reaction of oxygen with sulfur preadsorbed onto a Cu surface. He used this study to demonstrate the use of Auger spectroscopy in studying reaction rates. An example of his results is given in Figure 6.23. He supplemented the Auger analysis with mass spectral analysis of the absorbed gases. From this study Bonzel concluded that (1) fast surface reactions between S and O can be measured by Auger spectroscopy, (2) the kinetics and partial dependence of surface reactions indicated a Langmuir-Hinshelwood mechanism, and (3) as a consequence of high activation energies the reaction could be surface-diffusion controlled. Holloway and Hudson⁽¹¹⁵⁾ have studied the kinetics of the reaction of oxygen with nickel surfaces.

The adsorption and desorption of CO on metal and alloy surfaces have been studied by several authors.⁽¹¹⁶⁾ Studies were carried out down to -145°C and Auger measurements were coupled with LEED, work function measurements, and flash desorption.

Thomas and Haas⁽¹¹⁷⁾ measured the adsorption of alkali metals on Mo(110). Results for cesium are shown in Figure 6.24. Both cesium and rubidium adsorption saturate out at about one monolayer, defined as one adsorbed atom per substrate atom. Potassium, on the other hand, continues to deposit above 1.2×10^{15} , indicating multilayer adsorption. Auger spectroscopy is a sensitive measurement for K, Rb, or Cs. As few as 5×10^{12} ions/cm² were detected of Rb. However, AES on sodium was relatively insensitive.

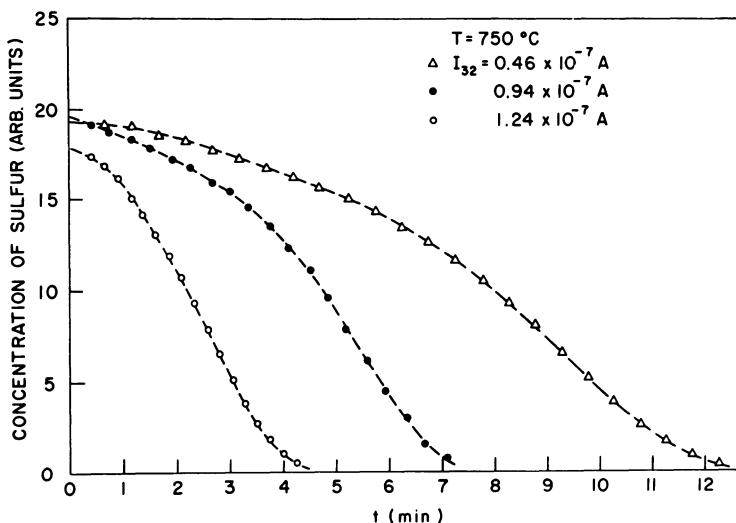


FIGURE 6.23. Concentration of adsorbed sulfur as a function of reaction time for constant temperature and partial pressure of oxygen. I_{32} is a direct measure of the partial pressure of oxygen. [Reproduced from Bonzel.⁽¹¹⁴⁾]

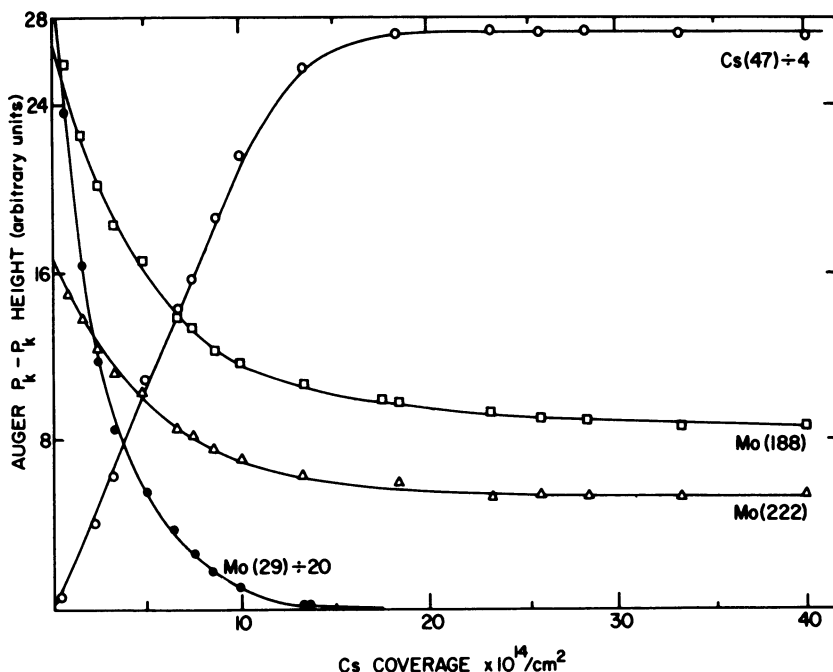


FIGURE 6.24. Variation of Cs and Mo Auger intensity as a function of Cs coverage of Mo(110) surface. [Reproduced from Thomas and Haas,⁽¹¹⁷⁾ Figure 2.]

Tarng and Wehner⁽¹¹⁸⁾ studied the deposition and sputter removal of molybdenum from Cu, Au, Al, and W surfaces. The sputtering yields of Mo from foreign surfaces are sometimes an order of magnitude lower than removal of molybdenum from itself; thus, caution must be used in employing ion bombardment for layer removal in determination of depth-composition profiles.

The general area of AES in the study of thin films has been reviewed by Weber,^(119, 120) who points out that analysis can be carried out successfully on insulators as well as metals and semiconductors. The silicon-oxygen ratios have been determined in spin-on glass films at various temperatures by Smith *et al.*⁽¹²¹⁾

4.4.2.3. Inhomogeneity between the Bulk and Surface. The inhomogeneity of a given material can be nicely studied by Auger spectroscopy. For example, rocks of geological interest may be studied in detail over their whole surface without breaking apart the sample. Such an analysis was carried out on lunar samples by Connell and Gupta.⁽⁸⁸⁾

Often the surface analysis of a supposedly homogeneous material is quite different than that of the bulk. Coad and Rivière⁽¹²²⁾ showed that carbon segregates to the surface of nickel foil and is present as Ni₃C below 673°K but

turns to graphite about 573–873°K. This kind of segregation often occurs with sulfur impurities in metals as the result of heat treatment and has been so measured by Auger spectroscopy,^(102, 103) as was mentioned earlier. Segregation of boron, sulfur, and nitrogen in iron has been measured by Bishop and Rivière.⁽¹²³⁾ It was further found that fracturing of steel occurs along grain boundaries containing antimony, these boundaries being only a couple of atomic layers thick. See, for example, the work of Marcus and Palmberg⁽¹²⁴⁾ in Figure 6.25, which shows the presence of antimony in embrittled steel. AES has been used to study various problems of interfaces, such as a glass fiber-resin interface,⁽¹²⁵⁾ the silicon–gold interface,⁽¹²⁶⁾ and the interaction between adsorbed sulfur ions and a two-dimensional copper sulfide phase.⁽¹²⁷⁾

Auger spectroscopy could also be employed for the study of slow diffusion, particularly where knowledge of a very sharp profile, the order of a monolayer, is required.

Ellis⁽¹²⁸⁾ has studied the segregation of S, C, and P impurities in the bulk to the surface of thorium at elevated temperatures. The composition of alloys at the surface as compared with the bulk has been determined with AES by several authors. Quinto *et al.*⁽¹²⁹⁾ found the composition of a binary solid solution of copper and nickel to be essentially the same at the surface as in the bulk. The composition of Cu–Al alloy, however, was found to change as a function of temperature.^(114, 130) Dooley⁽¹³¹⁾ studied the behavior of zircalloys and was able to correlate the surface analysis (both impurities and alloy composition) with previously established mechanical properties.

Narusawa *et al.*⁽¹²⁶⁾ studied the nature of the mixed-phase formation of Si–Au (100–300°C) in an oxidizing atmosphere. They concluded that the reaction induces a mixed phase almost identical with the Si–Au alloyed phase obtained by heat treatment in a high vacuum.

4.4.2.4. Radiation Damage. One of the problems in the use of a high-intensity, sharply focused electron beam is radiation damage. This problem can be turned to an advantage in the study of surface effects due to electron bombardment. For example, Palmberg and Rhodin⁽¹³²⁾ and later Tokutaka *et al.*⁽¹³³⁾ investigated the surface dissociation of KCl under electron irradiation. The desorbed neutral particles of K, Cl, and Cl₂ were measured by mass spectroscopy, while the surface concentration was analyzed by Auger spectroscopy. For temperatures above 60°C surface stoichiometry was maintained, but below that value there was a net loss of Cl. Desorption of adsorbed gases such as oxygen on tungsten⁽¹³⁴⁾ and CO on silicon⁽¹³⁵⁾ has been studied by Auger spectroscopy. In the latter case it was determined that the radiation damage occurred in a two-step process: (1) CO is dissociated and (2) the carbon diffuses over the surface while oxygen remains fixed. This was ascertained by monitoring different portions of the surface by Auger spectroscopy, but maintaining constant irradiation only at one point. Kirby and Lichtman⁽¹³⁶⁾ have recently

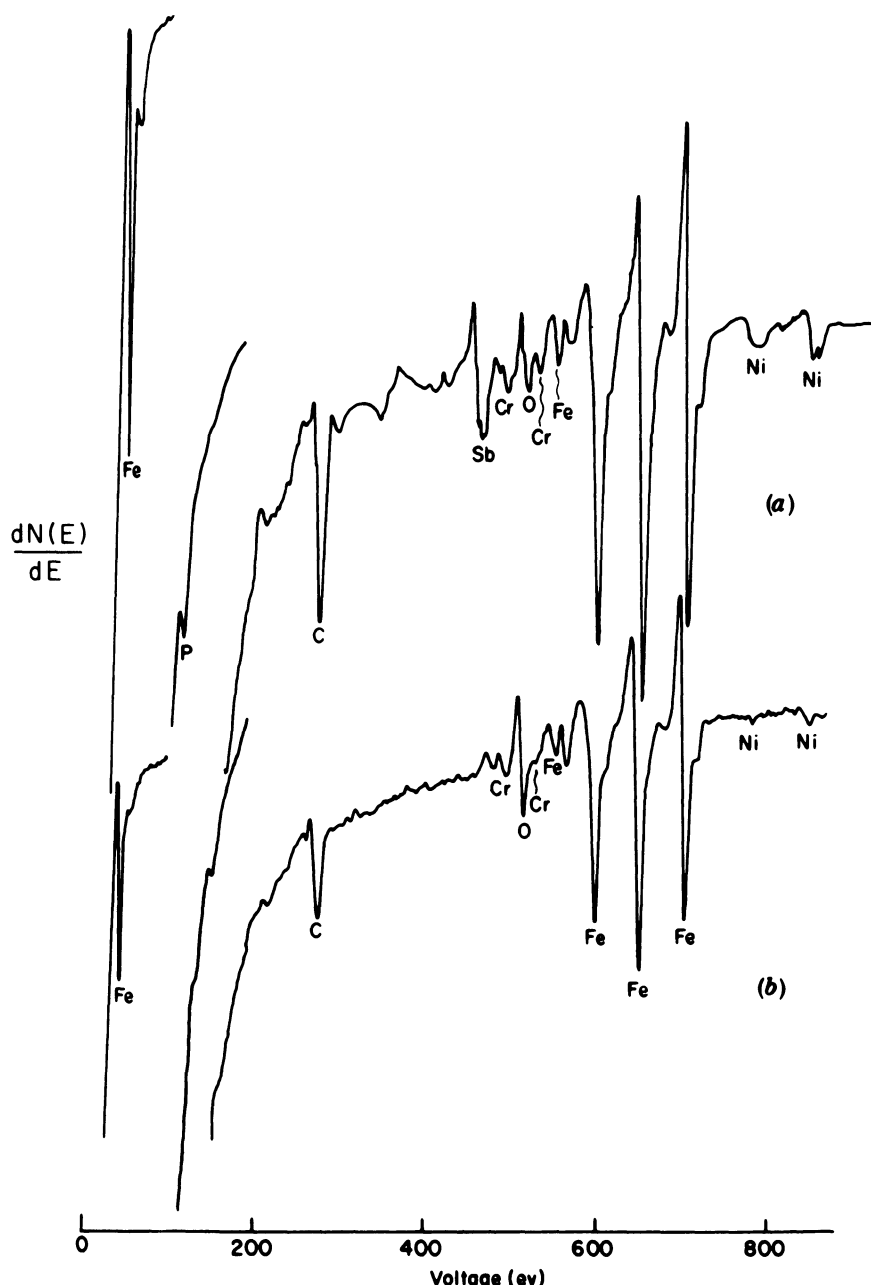


FIGURE 6.25. Auger spectra of fracture surface of AISI 3340 steel (a) embrittled, (b) unembrittled. [Reproduced from Marcus and Palmberg.⁽¹²⁴⁾]

extended the study of the effect of an electron beam on the gas adsorption of CO and O₂ on silicon.

Salmerón and Baró⁽¹³⁷⁾ observed chemical shifts in the Auger spectrum of silicon of SiO₂ due to reduction of the surface to silicon as the result of radiation damage.

4.4.2.5. Molecular Identification. As has been pointed out previously, Auger spectroscopy of solids is primarily used for elemental identification. But from studies on gases (cf. Figure 6.16) it is obvious that Auger spectra are also characteristic of the chemical environment. As high-resolution electron spectroscopy is used in surface studies, greater application to chemical bonding will be made. The chemical shifts measured in Auger spectroscopy are frequently not the same as experienced by core electrons measured in PESIS. This would require that the Auger transitions involve only electrons in the core shells. Rather, Auger "chemical shifts" quite often refer to transitions to the valence shell, so that one experiences not a simple change in the overall potential but a rather complicated alteration in the final state of the doubly charged molecular ions. (Again refer to Fig. 6.16.) These alterations sometimes result in a substantial change in the overall spectrum that can be easily measured even with an Auger spectrum of modest resolution. Interpretation of the chemical shift arising out of transitions to the valence shell is not straightforward, but molecular identification can be made once the spectrum of a pure compound has been measured. As pointed out earlier (Section 2), the differences between metals and dielectrics with regard to extraatomic relaxation can create a substantial chemical shift between the metal and its oxide. Most valuable for surface work are thus changes in the spectrum from the metal to its oxide or the identification of an adsorbed species.

Haas *et al.*⁽¹³⁸⁾ have presented a short review of the subject. From Table III of their paper one sees that shifts often can be correlated with electronegativity. In these cases Auger transitions usually involve core electrons. The shifts are similar to those found in PESIS, though slightly smaller. Grant and Haas⁽¹³⁹⁾ have used Auger spectroscopy to distinguish between the carbon in graphite and in silicon carbide. These authors⁽¹⁴⁰⁾ have also noted a chemical shift in the ruthenium Auger spectra as the result of the presence of carbon on the surface of ruthenium. Joyce and Neave⁽¹¹³⁾ found that the Auger spectrum for silicon oxidized on the surface at high temperatures was considerably different from that found with silicon having a high coverage of adsorbed oxygen, which indicated different chemical environments for the silicon. Chemical identification of mixtures of Be and BeO and of Al and Al₂O₃ have been made through their distinctive Auger spectra.⁽¹⁴¹⁾ For example, see Fig. 6.26.

LeJeune and Dixon⁽¹⁴²⁾ have offered an interpretation of oxidized beryllium in terms of total density of states. Szalkowski and Somorjai⁽¹⁴³⁾ have

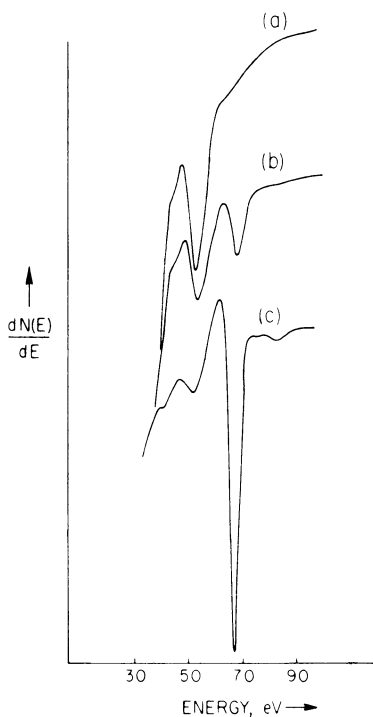


FIGURE 6.26. Auger spectra during progressive cleaning of pure Al sample. Curve (a) is essentially due to Al_2O_3 , (b) is due to $\text{Al} + \text{Al}_2\text{O}_3$, and (c) is due to "clean" Al. [Reproduced from Quinto and Robertson.⁽¹⁴¹⁾]

studied the chemical shifts of the $L_{\text{II}}-M_{\text{II},\text{III}}M_{\text{II},\text{III}}$ Auger transitions as a function of the oxidation state of vanadium, the surface composition of which was in turn ascertained from the Auger spectrum of oxygen. Chemical shifts between uranium oxide and its metal⁽¹⁴⁰⁾ and between Y and its oxide⁽¹⁴⁴⁾ have also been measured. It has been found that though chemisorption onto Pt⁽¹⁴⁶⁾ does not yield chemical shifts in the Auger energies, there is a decided modification of some of the Auger transition probabilities involving platinum valence electrons. Seo *et al.*⁽¹⁴⁷⁾ have studied the Auger chemical shifts of passive films and Dadayan *et al.*⁽¹⁴⁸⁾ have measured the shifts in the Auger spectrum of molybdenum and tungsten during oxidation.

Characteristic energy losses as Auger electrons emerge from the solid have been used to learn about the solid state structure of the material under study. Coad and Rivière⁽¹⁴⁹⁾ have used characteristic energy loss data combined with changes in the Auger spectrum to give information regarding the formation of surface oxide on Cr, V, Fe, and Co. Melles *et al.*⁽¹⁵⁰⁾ have measured characteristic energy losses in the Auger spectrum of phosphorus films.

When Auger transitions involve the valence band, one can in principle learn about the density of states from details of the Auger spectrum. This has been done for Mg_2Sn by Tejeda *et al.*⁽¹⁵¹⁾ and the results compared with photo-emission results using both XPS and UPS.

4.4.2.6. Combination of Auger Spectroscopy with Other Surface Techniques.

Auger spectroscopy is a particularly powerful tool when it can be combined with other techniques for studying the surface. Auger spectroscopy in fact received its initial impetus as the result of combining it with LEED. Low-energy electron diffraction gives information on the structure of the surface of a crystal. (It is restricted to measurements of a single crystal.) LEED is generally insensitive to the detection of impurities and gives information on structure, but not the elemental composition of the surface. Auger spectroscopy does this admirably and offers an ideal complement to LEED. For example, on cleaning Pt, a 1×5 pattern occurred in the LEED measurements, which was explained⁽¹⁵²⁾ with the help of Auger spectroscopy as due to the raising of oxygen impurities below the surface to close to the surface such as to cause an undulating surface and thus the 1×5 pattern.

Surface electrical properties of ZnO single crystals have been measured and correlated with LEED and Auger measurements.⁽¹⁵³⁾ Other examples of the use of Auger spectroscopy as a monitor for surface contamination during LEED studies are Jackson and Hooker's studies⁽¹⁵⁴⁾ on the deposition of Al onto Nb and Holcombe *et al.*'s investigation⁽¹⁵⁵⁾ of lithium hydride surface. For a review of Auger and LEED spectroscopies, see Tracy and Burkstrand.^(94c)

As with LEED, scanning electron microscopy utilizes an electron beam so that the opportunity for Auger spectroscopy is also provided simultaneously. As one maps the topographical features of a material by electron microscopy, one can also map the chemical composition of the surface by Auger spectroscopy. MacDonald and Waldrop⁽¹⁰⁰⁾ have given a particularly nice demonstration of the value of combining scanning electron microscopy with Auger spectroscopy, and have discussed its potentialities (cf. Figure 6.22). Griffiths *et al.*^(156, 157) have extended this discussion. Physical Electronics is now marketing an Auger microprobe. An x-ray emission microprobe has been for several years an important supplement to scanning electron microscopy. Let us make a few comparisons. X rays measure the bulk concentration better and are less sensitive to surface-cleanliness and high-vacuum requirements. An Auger microprobe sees the surface. Since the depth of material that is being probed is smaller, an Auger microprobe has a better ultimate resolution. More important, an Auger microprobe can study the very light elements, which cannot be handled by the x-ray emission microprobe.

Auger electron spectroscopy has also been combined with high energy electron diffraction, as, for example, in the work of Henderson and Helm,⁽¹⁵⁸⁾ who demonstrated that clean silicon surfaces could be grown in an even homoepitaxial manner by pyrolysis of SiH₄. A study was made of cesium adsorption on tungsten and titanium using the combined measurements of ellipsometry, Auger spectroscopy, and surface potential differences. The deposition of Cs⁺

did not occur unless some oxygen was detected on the sample by Auger spectroscopy.

An apparatus has been described by Palmberg in which surface chemical analysis by AES is carried out simultaneously with inert gas sputtering to obtain compositional profiles of the surface normal to the solid-vacuum interface. Robinson and Jarvis⁽¹⁵⁹⁾ have also used sputter etching with Auger spectroscopy to examine the alloying behavior of the Ni/Au-Ge Ohmic contact to *n*-type GaAs.

Nishijima and Murotani⁽¹⁶⁰⁾ have combined Auger electron spectroscopy with electron impact desorption (EID) in a study on silicon surfaces. Coad and Rivière⁽¹⁴⁹⁾ have used characteristic energy loss data combined with changes in the Auger spectrum to give information regarding the formation of surface oxide on Cr, V, Fe, and Co. Likewise, Kawai *et al.*⁽¹⁶¹⁾ have followed the oxidation of molybdenum surfaces by combining AES with energy loss spectroscopy. Willis *et al.*⁽¹⁶²⁾ have combined structure seen in the low-energy portion of the secondary electron energy distribution (3.0–17.5 eV) with Auger analysis to study carbon fiber surfaces.

Auger spectroscopy can be used successfully with a variety of other surface techniques: x-ray photoelectron spectroscopy in which both Auger and photoelectrons are produced in the same spectrum, high-energy electron spectroscopy for finding information regarding the structure of a material in the vicinity of the surface, and mass spectroscopy for analyzing desorbed gases and other particles ejected from the surface. Such an interweaving of these and other physical techniques has given rise to a substantial advance in the field of surface science.

4.5. Other Methods for Surface Analysis

During the recent development of Auger electron spectroscopy as an analytical tool for surfaces, other new methods have also been developed. First, we shall contrast AES with its closest counterpart, PESIS. Then we shall make brief mention of other miscellaneous physical techniques for chemical analysis of the surface.

4.5.1. Comparison of PESIS and Auger Spectroscopy for Surface Studies

The possible use of x-ray photoelectron spectroscopy for studying surfaces has been discussed in Chapter 5, Section 5.2. Comparison between the two techniques, photoelectron spectroscopy and Auger spectroscopy, for surface analysis has been made throughout this chapter. In this section I should like to tie this information together.

Both methods, PESIS and AES, study approximately the same portions of the surface. Although in principle an electron beam can produce a much stronger initial signal, in practice PESIS is almost as sensitive and in some cases more so when there is a large number of elements present. This is due in part to the better peak-to-background ratio found with photoionization as compared with electron bombardment, and with the fact that the limitation of sensitivity for surface detection lies ultimately more with surface cleanliness than with the sensitivity for measurement. Of course, Auger spectra can be obtained much faster, an important consideration if rapid changes on the surface are to be studied.

An important advantage of AES is that a beam with a highly focused spot can be used, so that the surface of a given material can be studied point by point, and AES may be used in conjunction with other surface-measuring devices such as LEED or electron microscopy. Somewhat offsetting these advantages is the care one must take with radiation damage of the sample being caused by an electron beam. In addition, there is the possibility of carbon deposits resulting from radiolysis of deposited hydrocarbon vapor (Chang^(94b) warns that the pressure due to hydrocarbon vapor should be held below 5×10^{-8} Torr). Also, there is the difficulty produced by charging of the sample if it is an insulator.

The chief advantage in using PESIS is that the spectra are simpler and easier to analyze, and that chemical shift measurements with their information concerning changes in the chemical environment are much easier to make and interpret. It is possible, however, in some cases to examine the nature of chemical shifts with Auger spectroscopy, and the importance of this should grow with application of high resolution analyzers.

Since both x-ray photoelectron spectroscopy and Auger spectroscopy can be carried out with the same electron spectrometer, it can be expected that in the future the two techniques will be used together frequently in the study of surface phenomena. For example, Coad and Cunningham⁽¹⁶³⁾ have combined the two techniques in the study of the oxidation of steel.

4.5.2. Methods of Surface Analysis Other than AES and PESIS

Gerlach *et al.*⁽¹⁶⁴⁾ have proposed the differentiation of the total integrated distribution (a total secondary electron yield) with respect to primary electron energy. What this accomplishes is a measurement of resonance absorption of core electrons into unfilled energy states above the Fermi level. This in turn identifies the atom by means of its binding energy. This method has been called ionization spectroscopy (IS).

Closely related to IS is appearance potential spectroscopy (APS), in which

x-ray fluorescence is measured at the ionization threshold of atomic levels by variation of the electron impact energy (see Ref. 165 for reviews). Musket⁽¹⁶⁶⁾ compared APS with Auger electron spectroscopy and found that AES is more sensitive for elemental analysis and that APS should be reserved for the study of chemical bonding of atoms on surfaces. Grant *et al.*⁽¹⁶⁷⁾ have combined AES and APS in their studies on titanium and titanium monoxide.

Secondary ion mass spectroscopy (SIMS) is a technique in which ions are sputtered off a surface and analyzed with a mass spectrometer. Under certain conditions SIMS is extremely sensitive. As few as parts per billion of alkali metals can be determined. Electron spectroscopy has, however, a much greater versatility for general analysis. For a comparison of the two methods, see Niehus and Bauer.⁽¹⁶⁸⁾ Examples⁽¹⁶⁹⁾ also exist of combining AES with SIMS.

Ion scattering spectrometry is (ISS) is a particularly important tool for surface work, since by its very nature it examines essentially only the outermost atomic layer (for a review of ISS, see Ref. 170). It operates simply on the conservation of energy and momentum, i.e.,

$$\frac{E_1}{E_0} = \frac{M_s - M_0}{M_s + M_0}$$

where E_0 and M_0 are the mass and kinetic energy of the impact ions, E_1 is the energy of the ion scattered at 90°, and M_s is the mass of the surface atoms. The mass analysis yields identification of the element. No information on chemical bonding is obtained, but studies on isotopic distribution are possible. The sensitivity is claimed to be approximately 1% of the surface monolayer for most elements. The samples studied must be reasonably flat, but all types of surface can be studied, from metals to insulators, either crystalline or amorphous.

Although new methods for surface analysis proliferate, Auger electron spectroscopy has proven itself highly versatile, reasonably sensitive, and capable of analyzing almost any element in the periodic table. It is unlikely that its usefulness for surface studies will not continue to grow.